

Hyper-distance Oracles in Hypergraphs

Giulia Preti
 Gianmarco De Francisci Morales
 Francesco Bonchi
 CENTAI, Italy

Abstract

We study point-to-point distance estimation in hypergraphs, where the query is parameterized by a positive integer s , which defines the required level of overlap for two hyperedges to be considered adjacent. To answer s -distance queries, we first explore an oracle based on the line graph of the given hypergraph and discuss its limitations: the main one is that the line graph is typically orders of magnitude larger than the original hypergraph.

We then introduce HYPED, a landmark-based oracle with a predefined size, built directly on the hypergraph, thus avoiding constructing the line graph. Our framework allows to approximately answer vertex-to-vertex, vertex-to-hyperedge, and hyperedge-to-hyperedge s -distance queries for any value of s . A key observation at the basis of our framework is that, as s increases, the hypergraph becomes more fragmented. We show how this can be exploited to improve the placement of landmarks, by identifying the s -connected components of the hypergraph. For this task, we devise an efficient algorithm based on the union-find technique and a dynamic inverted index.

We experimentally evaluate HYPED on several real-world hypergraphs and prove its versatility in answering s -distance queries for different values of s . Our framework allows answering such queries in fractions of a millisecond, while allowing fine-grained control of the trade-off between index size and approximation error at creation time. Finally, we prove the usefulness of the s -distance oracle in two applications, namely, hypergraph-based recommendation and the approximation of the s -closeness centrality of vertices and hyperedges in the context of protein-to-protein interactions.

1 Introduction

Computing point-to-point shortest-path distances is a key primitive in network-structured data [26], with widespread applications across various domains, including route planning [28], proximity search in databases [29], metabolic pathway analysis [62], web search ranking [77], and path finding in social networks [46]. The conventional approach to answering shortest-path queries involves using a single-source shortest-path algorithm for each query. However, this method leads to query times that grow linearly with the size of the network. An alternative approach involves an exhaustive computation of all possible queries through an all-pairs shortest-path algorithm, and storing these results in a lookup table. Yet, this method consumes a prohibitive amount of memory. In the context of real-world massive networks and with online applications requiring near-instantaneous point-to-point distances, these conventional approaches become impractical due to their prohibitively large query times or space requirements. For this reason, the research community has devoted large effort to developing *distance oracles* for approximate distance queries (see [67] for a survey). The key idea is to have an offline pre-processing phase in which an index is built from the network, and then an online querying phase in which the index is used to answer efficiently and approximately the distance queries.

In this paper, we tackle the problem of building distance oracles for *hypergraphs*, which are a generalization of graphs where an edge, called *hyperedge*, represents a q -ary relation among vertices. Hypergraphs are the natural data representation whenever information arises as set-valued or bipartite, i.e., when the entities to be modeled exhibit multi-way relationships beyond simple binary ones: cellular processes [63], protein interaction networks [21], VLSI [42], co-authorship networks [56], communication and social networks [71, 79], contact networks [9], knowledge bases [20], e-commerce [51], multimedia [1, 70], and image processing [11]. As taking into account polyadic interactions has been proven essential in many applications, mining and learning on hypergraphs has been gaining considerable research attention recently: researchers have developed methods for clustering and classification [33, 65], representation learning, structure learning and hypergraph neural networks [81, 22, 38], nodes classification and higher-order link prediction [6, 80, 34, 50], recommendation [37, 12, 82, 83], dense subgraphs and core/truss decomposition [13, 56, 60, 69].

Shortest paths in hypergraphs, or *hyperpaths*, have been used in many applications. [18] model a multichannel ad-hoc network as a hypergraph, where each hyperedge represents a group of nodes sharing a channel. Then,

a shortest hyperpath indicates the best route to transmit from source to destination. [24] represent the bus lines that are of interest for a passenger at a bus stop as a hyperedge, and a shortest hyperpath is a set of attractive origin-destination routes for that passenger. [48] use a hyperedge to capture a biochemical reaction among reactants, and a hyperpath is a series of reactions that start at receptors and end at transcription factors. Finally, [63] find the shortest hyperpaths in a hypergraph modeling protein interactions, to study which proteins and interactions stimulate a specific downstream response in a signaling pathway.

A path is a sequence of adjacent edges and, in graphs, two edges are *adjacent* if they share one vertex. As hyperedges can contain more than two vertices, a natural extension of the notion of adjacency to hypergraphs is to define two hyperedges adjacent if they share at least s vertices. The larger the value of s , the stronger the relation sought, because the larger is the amount of information (i.e., the vertices) shared between the hyperedges traversed. This notion of adjacency straightforwardly leads to the definition of s -*path*, i.e., a sequence of hyperedges such that consecutive hyperedges share at least s vertices. Previous work [3] shows that s -paths and s -connected components (i.e., hyperedges connected via s -paths) can unveil meaningful, interpretable, and significant structural insight within higher-order data. These insights are often disregarded when the data is modeled as a graph. For instance, when modeling signaling pathways as ordinary graphs, the representation falls short in capturing critical cellular activities involving the assembly and disassembly of protein complexes, multiway reactions among such complexes, or distinguishing between inactive and active forms of proteins or complexes [64]. Consequently, finding the shortest paths within the underlying graph of the cell-signaling network does not yield the most efficient ways for synthesizing a specific transcription factor from a set of receptors [45], and may even detect non-functional pathways [17].

Example 1. *Let us assume the hypergraph in Figure 1 (left) models contacts among people in an epidemiologic context. For $s = 1$, vertex 2 has the same distance from 7 and 9: in fact 2 belongs to hyperedge e_3 which is adjacent to e_6 (which contains both 7 and 9). While for $s = 2$, vertex 2 is closer to 7 (via hyperedge e_7 which has two vertices in common with e_3) than to 9, as e_6 is no longer adjacent to e_3 . As contacts are the cornerstone of the transmission of contagious diseases, if vertex 2 is infected, the chances that 7 is infected as well are higher than those of vertex 9, because 7 has a stronger connection to 2.*

Contributions and roadmap. We introduce a new type of point-to-point

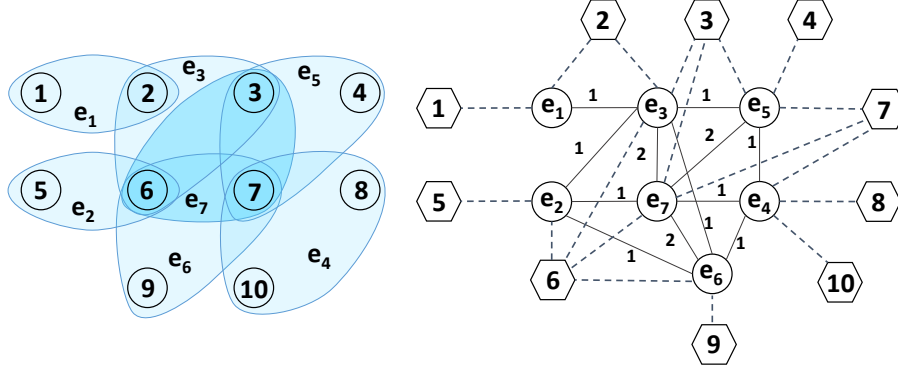


Figure 1: A hypergraph (left) and its line graph (right, see §4) augmented with hexagonal vertices and dashed edges to keep track of nodes-to-hyperedge membership.

distance queries in undirected hypergraphs, where a query is defined by the source, the target, and an integer s which indicates the desired level of overlap between consecutive hyperedges in a path. In particular, we consider variants of this type of query: vertex-to-vertex, hyperedge-to-hyperedge, and vertex-to-hyperedge. We show that the s -distance is a metric only for hyperedge-to-hyperedge queries, while for vertex-to-vertex it is a *semimetric*, as triangle inequality does not necessarily hold when $s > 1$. Moreover, vertex-to-vertex distance queries can be answered by finding the minimum distance between any two hyperedges that contain the given vertices, and similarly for vertex-to-hyperedge ones. We thus focus our oracle on hyperedge-to-hyperedge queries.

We show how a simple oracle can be obtained by means of a *line graph*, i.e., a graph representation of a hypergraph. In it, the hyperedges become vertices, and they have an edge between them if they share vertices in the hypergraph. However, this approach faces a major limitation in its scalability, as the line graph is typically orders of magnitude larger than the original hypergraph (§4). We thus introduce HYPED, a framework to build distance oracles with a desired size Q , expressed in terms of distance pairs stored by the oracle (§5.1). Our framework, like many others, is based on the concept of *landmarks*. In standard graphs, landmarks are vertices for which the oracle stores the distances to all the reachable vertices. Instead, HYPED uses hyperedges as landmarks. In contrast to graphs, hypergraphs encompass relations of varying orders, which necessitates the storage of a larger volume of information within the oracle to allow answering s -distance

queries for different values of s . One of the distinctive challenges in this endeavor is landmark selection. This task is notably more complex than in the case of graphs due to the substantial increase in the number of s -connected components as s grows. Consequently, a well-thought-out selection strategy that keeps into consideration the connectivity structure is essential to ensure that the oracle’s size remains within the user-defined limits and that it can approximate as many s -distances as possible. Note that this issue does not apply to the graph case, as the oracle is constructed solely for the giant connected component of the input graph. We thus devise an algorithm to compute the all the s -connected components of a hypergraph up to a max value s_{\max} (§5.2). Our algorithm combines a *union-find* technique [72], a dynamic inverted index, and a key property of the s -distance, to avoid redundant computations. Then, we devise and compare several different techniques to determine the number of landmarks to assign to each s -connected component (§5.3), and to select which hyperedges will act as landmarks for each component (§5.4). We compare HYPED against baselines (§6.2) and against line-graphs based methods (§6.3), to prove its effectiveness in estimating the distances, as well as its efficiency in creating the oracle and answering batches of queries. Finally, Section 6.4 and Section 6.5 prove the usefulness of the s -distance oracle in two applications, namely, hypergraph-based recommendation and the approximation of the s -closeness centrality of vertices and hyperedges in the context of protein-to-protein interactions.

2 Related Work

Distance queries in graphs. Distance oracles are compact representation of an input graph that enables to answer point-to-point shortest-path distance queries efficiently [26, 59, 67], and are assessed according to the space occupied and the query time. Approximate solutions aim at reducing the space required to store the oracle, with the downside of errors in the answer provided. [73] show that, for general graphs, one cannot have both a small oracle and a small error in the answers. Nonetheless, existing algorithms for general graphs with billions of nodes and edges have proven to be quite accurate and fast [61].

Even exact solutions may exploit precomputed structures. [2] propose a distance-aware 2-hop cover set (PLL), further parallelized by [39]. [78] optimize their index for answering batch queries. While the query time is smaller than that of PLL, the size of the index is much larger. [52] analyze the relation between graph tree width and PLL index size, and proposes a core-tree

index (CTL), with the goal of reducing the size requirements of PLL. The construction of the CTL index is based on a core-tree decomposition of the graph, which results in the identification of a forest of subtrees with bounded tree width and a large core. Finally, [19] construct a landmark-based index, used to get upper bounds to the distances at query time. The upper bounds are then used to speed up the computation of the actual distance, which uses a sparsified version of the graph.

Distance queries in hypergraphs. Shortest paths in hypergraphs have a long history in the algorithmic literature [24, 35, 58, 4] and in bioinformatics [63, 23, 48]. However, none of this work considers the problem of approximating shortest-path distance queries by means of an oracle.

[25] address the shortest path problem for weighted undirected hypergraphs, where paths can only be 1-paths. [66] focus on single-source shortest paths (SSSP) in weighted undirected hypergraphs and develops a parallel algorithm based on the Bellman-Ford algorithm for SSSP on graphs. Also in this case, only 1-paths are considered.

[3, 40] introduce the notion of s -walks, where s indicates the overlap size between consecutive hyperedges, and generalize several graph measures to hypergraphs, including connected components, centrality, clustering coefficient, and distance. These generalized measures are then applied to real hypergraphs to prove that they can reveal meaningful structures and properties, which cannot be captured by graph-based methods. As stated by the authors, the goal of their work is to discuss the need for ad-hoc analytic methods for hypergraphs, whereas the algorithmic aspects have not been taken into account (their analysis is on small hypergraphs up to 22k distinct hyperedges).

[15] consider higher-order connectivity in random k -uniform hypergraphs, i.e., hypergraphs whose hyperedges have all size k . [55] consider a slightly different notion of s -walks where the hyperedges intersect in exactly s vertices. Finally, [54, 53] propose parallel algorithms to construct the s -line graph of a hypergraph, as well as, an ensemble of s -line graphs for various values of s . The experimental evaluation on real-world hypergraphs confirms the hardness of the task, as the algorithm for the ensemble fails on most of the datasets due to memory overflow.

3 Preliminaries

We consider an undirected *hypergraph* $H \doteq (V, E)$ where $V = \{v_1, \dots, v_n\}$ is a set of vertices and $E = \{e_1, \dots, e_m\}$ is a set of *hyperedges*. Each hyperedge

Table 1: Notation.

Symbol	Description
$H \doteq (V, E)$	hypergraph
E_i	hyperedges of size no less than i
\mathcal{L}_s	s -line graph of H
\mathcal{L}	weighted line graph of H
\mathcal{L}_a	augmented line graph of H
s_{\max}	max value of s considered
CC	s -connected components of H up to s_{\max}
$\Delta_s(e, f)$	s -distance between $e, f \in E$
$\tilde{\Delta}_s(e, f)$	estimated s -distance $e, f \in E$
$\delta_s(u, v)$	s -distance between $u, v \in V$
$\tilde{\delta}_s(u, v)$	estimated s -distance between $u, v \in V$
$d_s(u, e)$	s -distance between $u \in V$ and $e \in E$
$\tilde{d}_s(u, e)$	estimated s -distance between $u \in V$ and $e \in E$
lb_s	lower-bound to Δ_s
ub_s	upper-bound to Δ_s
\mathcal{O}	distance oracle for H
Q	max desired oracle size
d_{\min}	min size of a connected component to be stored in the oracle
σ	landmark selection strategy

$e \in E$ is a set of vertices of cardinality at least 2, i.e., $e \subseteq V \wedge |e| \geq 2$. The cardinality of a hyperedge is also called *size*, while the *degree* of a vertex v is the number of hyperedges containing v . A *graph* is a hypergraph whose hyperedges have all cardinality equal to 2. Finally, given an integer i , we denote with E_i the subset of hyperedges with size not lower than i . Table 1 summarizes the most important notation.

In this paper, we adopt a notion of hyperedge adjacency parameterized by an integer s which indicates the minimum level of overlap between two hyperedges to be considered s -adjacent. This notion provides a natural and transparent interpretation of s as an association strength threshold and has been shown to provide meaningful structural insights about hypergraphs [3, 40]. More importantly for our problem, the s -distance between hyperedges defined in this manner is a metric [3]. This property enables the construction of accurate landmark-based oracles. In contrast, definitions of

hyperedge adjacency based on other set measures such as the Jaccard index lack metric properties, which hinders building accurate hyper-distance oracles. Furthermore, the Jaccard index tends to undervalue relationships between large and small hyperedges (even when one is contained in the other), and emphasizes relations among smaller hyperedges, potentially skewing the overall assessment of association strength.

Definition 1 (*s*-adjacent, *s*-walk, *s*-path [3]). *Given $s \in \mathbb{N}^+$, a *s*-walk of length $l \geq 2$ is a sequence of l hyperedges $[e_1, \dots, e_l]$ such that, for any $j \in [1, l-1]$, e_j and e_{j+1} are *s*-adjacent, that is, $|e_j \cap e_{j+1}| \geq s$. An *s*-path is a *s*-walk where for each $i \neq j \in [1, l]$ it holds that $e_i \neq e_j$. Two hyperedges e and f are *s*-connected iff there exists an *s*-path $[e, \dots, f]$.*

A 1-walk in the hypergraph in Figure 1 is $[e_1, e_3, e_5, e_6, e_3]$; a 2-walk is $[e_3, e_7, e_5, e_7, e_6]$; a 1-path is $[e_2, e_6, e_4]$; and a 2-path is $[e_3, e_7, e_6]$. Since the max overlap size between any two hyperedges is 2, the hypergraph is 3-disconnected. The pair of hyperedges $[e_3, e_7]$ is an example of 2-adjacent hyperedges, whereas $[e_1, e_3]$ are only 1-adjacent. We can easily see that a pair of *s*-adjacent hyperedges are also $(s-1)$ -adjacent.

Clearly, *s*-paths generalize graph paths to hypergraphs. In fact, a path in a graph is equivalent to a 1-path in the hypergraph representation of the graph, because any pair of adjacent edges in a graph path shares exactly 1 vertex. The existence of *s*-paths between hyperedges defines equivalence classes of hyperedges:

Definition 2 (*s*-connected components [3]). *Given a hypergraph H , a set of hyperedges $C \subseteq E$ is an *s*-connected component iff (i) there exists an *s*-path between any pair of hyperedges $e, f \in C$, and (ii) C is maximal, i.e., there exists no $J \supset C$ that satisfies the first condition. We say that H is *s*-connected iff there exists a single *s*-connected component, i.e., $C = E$.*

The number of hyperedges in C is also known as the *size* of C . The *density* of C is measured as the ratio between the number of *s*-adjacent hyperedges in C and the number of possible pairs of hyperedges in C , which is equal to $\binom{|C|}{2}$.

The *s*-distance between two hyperedges e and f , which we denote as $\Delta_s(e, f)$, is defined as the length of the shortest *s*-path between e and f , decreased by 1.¹ That is, the distance between two *s*-adjacent hyperedges

¹The *s*-distance is often defined as the length of the shortest *s*-path. We subtract 1 to align with graph theory conventions, where the distance between edges is the number of vertices in a shortest path between them, making adjacent edges connected by a path of length 2 but at distance 1.

is 1. Moreover, $\Delta_s(e, e) = 0$. If no s -path exists between e and f (i.e., they belong to different s -connected components), then $\Delta_s(e, f) = \infty$. If $|e| < s$, then $\Delta_s(e, f) = \infty$ for all $f \neq e \in E$.

Definition 3 (vertex-to-vertex s -distance). *The s -distance between two vertices $u, v \in V$ is*

$$\delta_s(u, v) \doteq \begin{cases} 0 & \text{if } u = v, \\ \min_{e_1 \ni u, e_2 \ni v} \Delta_s(e_1, e_2) + 1 & \text{otherwise.} \end{cases} \quad (1)$$

Definition 4 (vertex-to-hyperedge s -distance). *The s -distance between a vertex $u \in V$ and a hyperedge $e \in E$ is $d_s(u, e) \doteq \min_{e_1 \ni u} \Delta_s(e_1, e)$.*

While the s -distance between hyperedges is a metric [3], the s -distance between two vertices, or between a vertex and an hyperedge, is a *semimetric*, i.e., the triangle inequality does not necessarily hold when $s > 1$. As an example, let consider the hypergraph in Figure 1 (left). We can see that $\delta_2(1, 4) = \infty$, because there is no 2-path between hyperedges containing 1 and 4. In fact, only e_1 contains vertex 1, and the maximum overlap between e_1 and any other hyperedge is 1. In contrast, $\delta_2(2, 4) = 3$, thanks to the 2-path $[e_3, e_7, e_5]$; and $\delta_2(1, 2) = 1$, thanks to the common hyperedge e_1 . Since $\delta_2(1, 4) > \delta_2(1, 2) + \delta_2(2, 4)$, the measure δ_s does not satisfy the triangle inequality.²

²An alternative definition of vertex-to-vertex s -distance that is a metric could be considered. Let the dual hypergraph be the one obtained by swapping the roles of vertices and hyperedges: hyperedges become vertices, and each vertex in the original hypergraph becomes a hyperedge that connects all the vertices in the dual that correspond to the hyperedges of the original hypergraph by which it was contained. We can compute the hyperedge-to-hyperedge s -distance in this dual hypergraph and obtain a metric vertex-to-vertex s -distance in the original hypergraph.

However, note that the vertex-to-vertex s -distance as in Definition 3 and the hyperedge-to-hyperedge s -distance in the dual hypergraph yield distinct results. For instance, s -connected vertices in the hypergraph may be at infinite distance in the dual. In fact, an s -path in the hypergraph is a sequence of hyperedges such that consecutive hyperedges share at least s common vertices, whereas an s -path in the dual is a sequence of vertices such that consecutive vertices belong to at least s common hyperedges.

Both definitions are valid and could be adopted depending on the applications at hand. Our framework can also handle this alternative definition of vertex-to-vertex s -distance, by simply applying it to the dual hypergraph. Of course, this leads to a separate oracle which could not be used to answer hyperedge-to-hyperedge s -distance queries in the original hypergraph. Therefore, henceforth we focus on the vertex-to-vertex s -distance as per Definition 3. This allows to answer all three types of queries with a single oracle.

Given that hyperedge-to-hyperedge distance is the basis for computing also the other two types of queries, we focus our attention on building oracles for this type of distance query, i.e., given $e, f \in E$ and $s \in \mathbb{N}^+$, return, as fast as possible, $\Delta_s(e, f)$ or a good approximation $\tilde{\Delta}_s(e, f) = \Delta_s(e, f) + \epsilon$ with $\epsilon \approx 0$.

In many applications, the best value of s might not be specified; on the contrary, the user might be interested in understanding how close two entities are for different values of s . For instance, in recommender systems one may want to rank the results of the queries trading-off between distance and overlap size: a close entity for a small s may be as relevant as an entity which is more distant, but for a larger s . In these cases, especially if the connectivity and the dimension of the hypergraph are not known apriori, the user needs to ask several queries with different values of the parameter s . For this reason, we study a more general problem, i.e., to compute the *distance profile* of e and f :

Problem 1 (distance profiling). *Given $e \neq f \in E$, compute $\Delta_s(e, f)$ for all $s \leq \min(|e|, |f|)$.*

The stopping threshold for the distance profiles derives from the fact that for all $s > \min\{|e|, |f|\}$, $\Delta_s(e, f) = \infty$.

This problem can be solved at query time, by executing a bidirectional BFS for each value of s . This strategy, however, leads to large query times; hence it is not viable for real-time query-answering systems. A common approach for fast query-answering is to pre-compute all the distance pairs and store them in a distance table. This approach, however, requires to store a huge amount of information, and hence is characterized by high space complexity. A trade-off between time and space is represented by the so-called *distance oracle*. A distance oracle is a data structure that stores less information than a distance table, but allows a query to be answered faster than executing a BFS. Distance oracles can be designed to answer queries either exactly or approximately. In line with the literature on shortest path queries in graphs, we opt for approximate in-memory solutions, to further reduce the space complexity [32].

4 Line-graph based oracle

One of the tools widely used in hypergraph analysis is the *line graph*, which represents hyperedges as vertices and intersections between hyperedges as edges:

Definition 5 (line graph [7]). Let $H = (V, E)$ be a hypergraph. The line graph of H , denoted as $\mathcal{L}(H)$, is the weighted graph on vertex set E and edge set $\{(e, f) \subseteq E \times E \mid e \neq f \wedge |e \cap f| \geq 1\}$. Each edge (e, f) has weight $\omega(e, f) = |e \cap f|$.

The s -line graph of H , denoted $\mathcal{L}_s(H)$, is its line graph from which only edges with weight at least s are retained. It is straightforward to see that the s -distance $\Delta_s(e, f)$ between two hyperedges e and f in the hypergraph H , corresponds to the distance between their corresponding vertices in the s -line graph $\mathcal{L}_s(H)$.

Example 2. Figure 1 shows an hypergraph (left) and its corresponding line graph (right) augmented with a vertex for each vertex in the hypergraph (denoted with hexagons) and an edge for each vertex-to-hyperedge membership (denoted with dashed lines). We can easily verify that the distance between e_3 and e_5 in the 2-line graph is 2 (they are connected via the shortest path $[(e_3, e_7), (e_7, e_5)]$ of edges with weight ≥ 2), while $\Delta_2(e_3, e_5) = 2$ (via the 2-path $[e_3, e_7, e_5]$).

This observation hints a way to produce a distance oracle for a given hypergraph H based on its line graph $\mathcal{L}(H)$. At query time, given hyperedges e and f and the desired value of s , one can obtain $\mathcal{L}_s(H)$ from $\mathcal{L}(H)$, retrieve the vertices corresponding to e and f and compute their distance in $\mathcal{L}_s(H)$. As the line graph is a standard graph, one can preprocess it to build a distance oracle using any state-of-the-art method for graphs (see experiments in Section 6.2).

Limitations. The main limitation of such an approach is that line graphs are typically much larger than the original hypergraphs, as their number of edges is in the order of $O(d_{\text{MAX}}^2)$, where d_{MAX} is the max number of s -adjacent hyperedges of a hyperedge in H . The complexity worsens when we need to answer also vertex-to-vertex s -distance queries: in this case, the line graph needs to be augmented with a new vertex u_v for each $v \in V$, and a new edge between u_v and each vertex in the line graph that corresponds to a hyperedge including v (see Figure 1 (right)). As a consequence, the augmented line graph has $|V| + |E|$ vertices of different types (those denoted with circles and those with hexagons in Figure 1), and up to $|V||E| + d_{\text{MAX}}^2$ edges.

Table 2 reports several statistics for 8 real-world hypergraphs: number of vertices, number of hyperedges, number of vertices and edges in the line graph, number of vertices and edges in the augmented line graph, disk usage of the hypergraph, and disk usage of the line graph. On average, the line

Table 2: Number of nodes and hyperedges in the hypergraph $H = (V, E)$, number of edges in the corresponding line graph \mathcal{L} , number of nodes and number of edges in the corresponding augmented line graph \mathcal{L}_a , disk size of H (DS_H), and disk size of \mathcal{L} ($DS_{\mathcal{L}}$).

Dataset	$ V $	$ E $	$ E_{\mathcal{L}} $	$ V_{\mathcal{L}_a} $	$ E_{\mathcal{L}_a} $	DS_H	$DS_{\mathcal{L}}$
NDC-C	1.1K	1K	36K	2.2K	42K	28K	1.2M
ETFs	2.3K	2K	47K	4.5K	53K	28K	444K
High	327	8K	593K	8.1K	611K	72K	5.8M
Zebra	10K	10K	104K	20K	154K	352K	3.3M
NDC-S	5.3K	10K	2.4M	15K	2.4M	256K	33M
Primary	242	13K	2.2M	13K	2.3M	152K	23M
Enron	50K	106K	153M	156K	153M	1.6M	1.9G
Epinions	756K	107K	32M	863K	46M	90M	944M
DBLP	1.9M	2.4M	125M	4.4M	133M	51M	2G
Threads-SO	2.7M	7M	263M	9.6M	277M	99M	3.9G

graph has 238x more edges than the related hypergraph has hyperedges, with Enron being the hypergraph with the largest increase (1435x). Similarly, the augmented line graph has 254x more edges, on average. Consequently, a distance oracle built on top of a line graph may require significantly more space. A second issue with a line-graph-based solution is that creating the line graph is a challenge in itself. Few approaches have been proposed in the literature, which, however, aim at generating the s -line graph for a given s [54], and hence require a considerable amount of redundant work to obtain all the s -line graphs up to a max s_{\max} . A third issue is that the state-of-the-art distance oracles for graphs are not designed to consider two different types of vertices, as it is the case with the augmented line graph needed to answer vertex-to-vertex s -distance queries. Thus, their adoption would not be straightforward in this case (in fact, in Section 6.2 we experiment with the line-graph-based approach only for hyperedge-to-hyperedge queries). Finally, the fidelity of line graphs in accurately representing hypergraphs remains uncertain, as demonstrated by Kirkland [44]: instances exist where non-isomorphic hypergraphs yield identical weighted line graphs. Consequently, oracles built on top of line graphs might result in less accurate distance approximations, especially for specific types of hypergraphs.

5 Landmark-based oracle

In light of the limitations discussed above, we propose an approach based on the idea of *landmarks* [59] that allows building oracles of a predefined size that operate directly on the hypergraph, thus avoiding going through its line graph.

In the standard graph setting, given a set of *landmark* vertices $L \subset V$, a distance oracle is built by storing the exact distances $d(l, u)$ from each landmark $l \in L$ to each vertex $u \in V$. Therefore, a larger number of landmarks implies a higher space complexity. Then, the approximate distance $\hat{d}(u, v)$ between u and v is given by $\hat{d}(u, v) = \min_{l \in L} d(l, u) + d(l, v)$. Since the distance between graph vertices is a metric, the approximate distance satisfies $\hat{d}(u, v) \geq d(u, v)$, and hence constitutes an upper bound to the real distance. In addition, a lower bound to $d(u, v)$ can be computed as $\max_{l \in L} |d(l, u) - d(l, v)|$.

In our setting, one first key idea is to use hyperedges, instead of vertices, as landmarks. Recall in fact that, in hypergraphs, only the hyperedge-to-hyperedge distance satisfies the triangle inequality, a crucial property for landmark-based solutions. The second key idea is to select different sets of landmarks for different values of the parameter s . Figure 2 shows how the connectivity of several real-world hypergraphs changes as the value of the parameter s increases. For $s = 1$, the hypergraphs are almost connected, but as s increases, the hyperedges form smaller s -connected components. As a consequence, a set of landmarks selected for a certain s may not be effective enough for approximating the $(s+1)$ -distances. This fact motivates the need for different sets of landmarks.

Next, we introduce our framework, HYPED (Hypergraph Estimation of s -Distances), which exploits a connectivity-based landmark assignment strategy and the topology of the s -connected components of the hypergraph, to construct a landmark-based distance oracle with predefined size. Finally, we discuss its complexity in Section 5.5.

5.1 The HYPED Framework

HYPED (Algorithm 1) bases its landmark selection on the s -connected components CC of H , given an integer s_{\max} , the maximum value of the parameter s for which to estimate the s -distances.

Offline phase: oracle construction. The first step is the computation of CC (Algorithm 2). Then, the oracle stores, for each $e \in E$ and each $s \leq \min([s_{\max}, |e|])$, the id of the s -connected component that includes e .

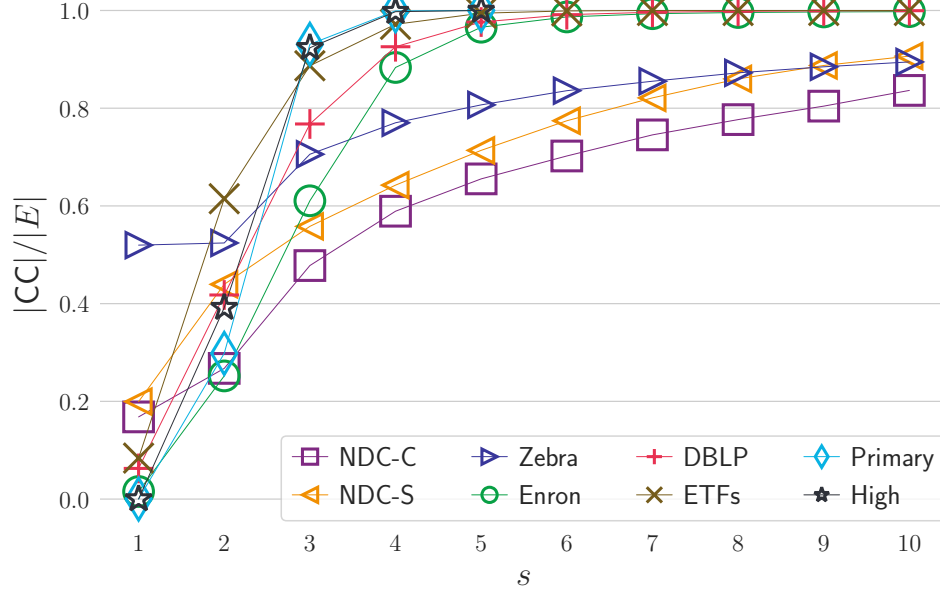


Figure 2: Number of s -connected components $|CC|$ (normalized to the number of hyperedges $|E|$) as a function of s . Lower values indicate higher connectivity.

Algorithm 1 HYPED

Require: Hypergraph H , Max s s_{\max}
Require: Min Dim d_{\min} , Max Oracle Size Q
Require: Importance Factors Ω
Require: Landmark Selection Strategy σ
Ensure: Distance Oracle \mathcal{O}

- 1: $\mathcal{O}.CC \leftarrow \text{FINDCONNECTEDCOMPONENTS}(H, s_{\max})$
- 2: $\mathcal{O}.AVGD \leftarrow \emptyset$
- 3: **for** $i \in [2, d_{\min}]$ **do** $\mathcal{O}.AVGD[i] \leftarrow \text{APPROXAVGDIST}(i)$
- 4: $L \leftarrow \text{SELECTLANDMARKS}(\mathcal{O}.CC, Q, d_{\min}, \Omega, \sigma)$
- 5: **for** $s \in [1, s_{\max}]$ **do** $\mathcal{O}[s] \leftarrow \text{POPULATEORACLE}(H, L[s], s)$
- 6: **return** \mathcal{O}

At query time, this information speeds up the distance estimation for hyperedges in different components.

For small s -connected components, the s -distance between their hyperedges can be bounded by a small constant. Therefore, it can be approximated accurately without using landmarks, by exploiting their topology (e.g., wedge, triangle, star). Knowing the topology of a component c al-

Algorithm 2 FINDCONNECTEDCOMPONENTS

Require: HyperGraph H , Max s s_{\max} **Ensure:** Connected Components \mathbf{CC}

```
1:  $I \leftarrow \emptyset; \mathbf{OP} \leftarrow \emptyset; \mathbf{CP} \leftarrow \emptyset$ 
2: for  $s \in [s_{\max}, 1]$  do
3:    $E_s \leftarrow \{e \in E \text{ s.t. } |e| \geq s\}$ 
4:    $\tilde{\mathbf{CC}} \leftarrow [\{e\} \text{ for each } e \in E_s]$ 
5:   initialize  $\tilde{\mathbf{CC}}$  using  $\mathbf{CC}_{s+1}$ 
6:   for  $e \in E_s$  not indexed yet do
7:     for  $v \in e$  do  $I[v] \leftarrow I[v] \cup \{e\}$ 
8:    $\mathbf{OV} \leftarrow \emptyset$ 
9:   for  $v \in I$  do
10:    for  $(e_1, e_2) \in I[v]$  do
11:      if  $e_1$  and  $e_2$  are not in the same  $c \in \tilde{\mathbf{CC}}$  then
12:         $\mathbf{OV}[(e_1, e_2)] \leftarrow \mathbf{OV}[(e_1, e_2)] + 1$ 
13:        if  $\mathbf{OV}[(e_1, e_2)] \geq s$  then
14:           $\mathbf{OP} \leftarrow \mathbf{OP} \cup \{(e_1, e_2, \mathbf{OV}[(e_1, e_2)])\}$ 
15:           $\tilde{\mathbf{CC}} \leftarrow \text{UNIONFIND}(\tilde{\mathbf{CC}}, e_1, e_2)$ 
16:        else  $\mathbf{CP} \leftarrow \mathbf{CP} \cup \{(e_1, e_2)\}$ 
17:    $\mathbf{CC}[s] \leftarrow \tilde{\mathbf{CC}}$ 
18: return  $\mathbf{CC}$ 
```

Table 3: Approximate distances in topologies with different numbers of elements n and connections m .

n	m						
	$n-1$	n	$n+1$	$n+2$	$n+3$	$n+4$	$n+5$
2	1						
3	1.3	1					
4	1.55	1.3	1.16	1			
5	1.8	1.58	1.42	1.3	1.2	1.1	1

allows us to exactly compute the average distance between its hyperedges. However, the identification of the topology of c is a hard problem known as *graph isomorphism*. To reduce the time and space complexity of our approach, we estimate the approximate distance between hyperedges in c as the expected average distance between pairs of hyperedges across topologies with the same size of c , and store a value for each size i up to a max integer d_{\min} (Algorithm 1 Line 3). For example, for $|c| = 3$ there are two topologies: the wedge and the triangle. In the former, the average distance between pairs of nodes is 1.33, while in the latter, it is 1. Therefore, the approximate distance is 1.16. This computation is doable for topologies with up to 5 hyperedges, as they can be easily enumerated, and their pairwise distances can be easily listed. The approximate distances for topologies with n elements and m connections is reported in Table 3. We observe that

in the online phase, if the algorithm has access to the input hypergraph, distances between hyperedges in small s -connected components can be efficiently computed using bidirectional BFSs. However, in our case, we assume that during query time, we only have access to the distance oracle.

For each s -connected component of size larger than d_{\min} , the subroutine SELECTLANDMARKS assigns a budget of landmarks and selects them. In particular, HYPED takes as input a desired oracle size Q indicating the maximum number of distance pairs that we are willing to store in the oracle. This threshold is used to select the appropriate amount of landmarks in the s -connected components. Finally, given the sets of landmarks L_s for each $s \leq s_{\max}$, the oracle finds and stores the exact s -distance between each $l \in L_s$ and each $e \in E_s$ reachable from l (Algorithm 1 Line 5).

Online phase: estimating the distance profile. Given the sets of landmarks L_s selected for each s of interest, HYPED computes the lower (lb_s) and upper (ub_s) bounds to the s -distance between any pair of hyperedges e and f as follows:

$$\text{lb}_s(e, f) = \max_{l \in L_s} |\Delta_s(l, e) - \Delta_s(l, f)| \quad (2)$$

$$\text{ub}_s(e, f) = \min_{l \in L_s} (\Delta_s(l, e) + \Delta_s(l, f)) \quad (3)$$

Then, it generates the distance profile of e and f , by computing, for each $s \in [1, s_{\max}^*]$ with $s_{\max}^* = \min(s_{\max}, |e|, |f|)$, the approximate s -distance $\tilde{\Delta}_s(e, f)$ as:

$$\tilde{\Delta}_s(e, f) = \begin{cases} \infty & \text{if } e \in c_i^s \wedge f \in c_j^s \wedge i \neq j, \\ \text{AVGD}(|c^s|) & \text{if } e, f \in c^s \wedge |c^s| \leq d_{\min}, \\ \frac{(\text{lb}_s(e, f) + \text{ub}_s(e, f))}{2} & \text{otherwise.} \end{cases}$$

where AVGD is the average pairwise distance in a graph with $|c^s|$ vertices, computed in Algorithm 1 Line 3.

Given two query vertices u and v , the distance profile of u and v is obtained by calculating the approximate s -distance $\tilde{\delta}_s(u, v)$, for each $s \in [1, s_{\max}^*]$ with $s_{\max}^* = \min(s_{\max}, |e^u|, |e^v|)$, with e^u (e^v) being the largest hyperedge including u (v), as:

$$\tilde{\delta}_s(u, v) = \min_{e \ni u, f \ni v} \tilde{\Delta}_s(e, f).$$

The approximate s -distances are further refined based on the following observation:

Observation 1. For any $e, f \in E$,

$$\Delta_s(e, f) \leq \Delta_{s+1}(e, f).$$

In particular, the lower-bound $\text{lb}_s(e, f)$ for $s \in [2, s_{\max}^*]$ can be improved as $\text{lb}_s(e, f) = \max(\text{lb}_s(e, f), \text{lb}_{s-1}(e, f))$; while the upper-bound $\text{ub}_s(e, f)$ for $s \in [1, s_{\max}^* - 1]$ can be improved as $\text{ub}_s(e, f) = \min(\text{ub}_s(e, f), \text{ub}_{s+1}(e, f))$.

5.2 Finding the s -Connected Components

The s -connected components of the hypergraph are a key factor for the selection of landmarks. Their computation is the bottleneck of the offline phase of our algorithm. For this task, we propose a technique that combines the *union-find* approach [72] and a dynamic inverted index, while exploiting Observation 1. We first describe how union-find works, and then explain our technique, which is outlined in Algorithm 2.

Union-find algorithms have been successfully applied to find connected components in graphs [57]. Here we describe a more advanced version with two types of optimizations.

Given a set of vertices V and a set of edges E , it iterates over the edges to find disjoint sets of connected vertices, i.e., groups of vertices connected via paths, but isolated from each other. The underlying data structure is a forest, where each tree represents a connected set, and each vertex is associated with (i) a *rank* initially set to 0 and (ii) a pointer to the parent. Each vertex starts as a tree by itself and hence points to itself. Then, the connected components are found via the application of two operators: *union-by-rank* and *find* enhanced with *path compression*. Given an edge (u, v) , *union-by-rank* merges the tree of u and that of v , based on the rank associated to their root: if the rank is different, the root with lowest rank is set to point to the other root; if the two ranks are equal, one of the roots is set to point to the other one, and the rank of the latter is increased by 1. Given a vertex u , *find* returns the root of the tree of u , and, for all the vertices traversed, sets their pointer to the root. This way, any subsequent *find* for these vertices will be faster.

Algorithm 2. According to Observation 1, if two hyperedges are in the same s -connected component, they also belong to the same $(s-1)$ -connected component. Therefore, we search for the s -connected components in decreasing order of s , so that the s -connected components can be used to initialize the $(s-1)$ -connected components (Line 5). The dynamic inverted index I

stores, for each vertex v , the hyperedges including v . This index is updated at each iteration s , including the hyperedges e not yet considered, i.e., those with size s (Line 7). Thanks to I , we can examine only pairs of hyperedges that actually overlap. The partial overlap is stored in a dictionary OV . Each time a pair (e_1, e_2) is considered, we first check if we already know that they belong to the same connected component. This can happen in two cases: (i) e_1 and e_2 belong to the same $(s+1)$ -connected component, or (ii) union-find merged their trees in a previous call. If this is not the case, we update their partial overlap (Line 12). If the overlap exceeds the min overlap size s , then e_1 and e_2 are s -connected, and hence we can call $UNION-FIND$ to propagate this information and update \tilde{CC} . During the search of the s -connected components, we discover partial overlaps $OV[(e_1, e_2)]$ between pairs of hyperedges. In addition, thanks to the transitive property, we may find that two hyperedges belong to the same s -connected component, without computing their overlap. We store these pairs in a set CP , and the partial overlaps in a set OP . These sets are exploited in the initialization of the sets of s -adjacent hyperedges, which are needed to find the s -distances between hyperedges. In particular, if the partial overlap between two hyperedges is $OV[(e_1, e_2)] = o$, then, e_1 and e_2 are s -adjacent for each $s \leq o$. Conversely, for each pair of hyperedges in CP , we need to compute their overlap, as we only know that they are s -connected but not whether they are s -adjacent. To save space, we do not explicitly store the s -connected components of hyperedges with size lower than s , as such hyperedges are s -disconnected from the rest of the hypergraph. The oracle can still compute the vertex-to-vertex s -distance between vertices in the same hyperedge of size lower than s , thanks to a vertex-to-hyperedge map created at query time. This map stores, for each vertex, the ids of the hyperedges containing that vertex. This way, we can determine the 1-hop neighbors of each vertex.

Next, we show how $HYPED$ exploits the s -connected components to guide the landmarks assignment and selection process. It explicitly divides the process into two phases: a landmark assignment (LA) phase, where the goal is to find the number of landmarks l_c to assign to each s -connected components c , for each $s \in [1, s_{\max}]$; and a landmark selection (LS) phase, where the goal is to select, for each component c , l_c hyperedges as landmarks. As discussed previously, only the connected components with size greater than the lower bound d_{\min} are taken into consideration.

5.3 Landmark Assignment

We propose two different strategies for the LA phase: a sampling-based strategy and a ranking-based one. Both strategies require the set $\text{CC} = \{\text{CC}_1, \dots, \text{CC}_{s_{\max}}\}$ with $\text{CC}_i = \{c_1^i, \dots, c_{|\text{CC}_i|}^i\}$ of s -connected components up to a maximum value s_{\max} , the target oracle size Q , and a set of importance factors Ω . These strategies assign a number of landmarks to each s -connected component, such that the total size of the oracle is bounded by Q . Once the assignment is found, the selection of the landmarks within each component (LS phase) is executed according to a strategy σ (Section 5.4).

The following observation tells us that the assignment strategy should prioritize larger connected components:

Observation 2. *The larger a connected component c , the higher the probability that a distance query involves two hyperedges in c .*

Furthermore, the following observation suggests that connected components with more vertices should be preferred:

Observation 3. *Given equal number of hyperedges, the more the vertices in a connected component c , the sparser is c , the higher the probability that each hyperedge covers a lower number of shortest paths.*

In fact, the lower the number of vertices in the connected component c , the more the hyperedges in c overlap with each other, and therefore, the shortest paths in c are more likely to include the same hyperedges. As a consequence, the denser is c , the lower the number of hyperedges needed to cover all the shortest s -paths in c . As shown in Section 5.4, the number of shortest paths covered by a hyperedge is a good indicator of its suitability as landmark.

Sampling-based strategy. The sampling strategy assigns a probability $\mathbb{P}_{c^s} \in [0, 1]$ to each s -connected component c^s , and iteratively samples a connected component from CC , until the estimated oracle size Q_{est} reaches the target size Q . When an s -connected component c^s is sampled, an additional landmark is assigned to c^s only if the number of landmarks already assigned to c^s is lower than $|c^s|$ (there cannot be more landmarks than hyperedges in c^s). If the landmark is assigned to c^s , Q_{est} is updated by adding $|c^s|$, because the oracle will store the distances from the landmark to every hyperedge in c^s . Let $\alpha \geq 0$ be the importance factor of the s -component size, $\beta \geq 0$ s.t. $\alpha + \beta \leq 1$ be the importance factor of the value s for which the component is a s -connected component, and $1 - (\alpha + \beta)$ the importance

Algorithm 3 SELECTLANDMARKS

Require: Connected Components CC , Max Oracle Size Q

Require: Min Dim d_{\min}

Require: Importance Factors Ω

Require: Landmark Selection Strategy σ

Ensure: A set of landmarks $L[s]$ for each s

```
1:  $C^{d_{\min}} \leftarrow$  connected components  $c$  with  $|c| > d_{\min}$ 
2:  $r_1 \leftarrow C^{d_{\min}}$  ranked by decreasing size
3:  $r_2 \leftarrow C^{d_{\min}}$  ranked by decreasing num of vertices
4:  $r_3 \leftarrow C^{d_{\min}}$  ranked by decreasing  $s$ 
5:  $r_4 \leftarrow C^{d_{\min}}$  ranked by increasing landmarks assigned
6:  $Q_{\text{est}} \leftarrow 0$ ;  $L \leftarrow \emptyset$ 
7: while  $Q_{\text{est}} < Q$  do
8:    $\text{RANK} \leftarrow \text{AGGRANKING}(r_1, r_2, r_3, r_4, \Omega)$ 
9:   take a random  $c^s$  in the first position of  $\text{RANK}$ 
10:   $L[s] \leftarrow L[s] \cup \text{SELECTLANDMARK}(c^s, L, s, \sigma)$ 
11:   $Q_{\text{est}} \leftarrow Q_{\text{est}} + |c^s|$ 
12:  if  $|c^s|$  landmarks have been assigned to  $c^s$  then
13:    remove  $c^s$  from the rankings
14:  else update  $r_4$ 
15: return  $L$ 
```

factor of the number of vertices in the s -connected component. Therefore, the larger is α , the more important the size of the s -component over s and its number of vertices.

Then, the sampling probability \mathbb{P}_{c^s} of c^s is

$$\mathbb{P}_{c^s} = \alpha \frac{|c^s|}{\zeta(\text{CC})} + \beta \frac{s}{\eta(\text{CC})} + (1 - \alpha - \beta) \frac{|V_{c^s}|}{\xi(\text{CC})} \quad (4)$$

where

$$\zeta(\text{CC}) = \sum_{i=1}^{s_{\max}} \sum_{j=1}^{|\text{CC}_i|} |\text{CC}_{i,j}|, \quad \xi(\text{CC}) = \sum_{i=1}^{s_{\max}} \sum_{j=1}^{|\text{CC}_i|} |V_{\text{CC}_{i,j}}|,$$
$$\text{and } \eta(\text{CC}) = \sum_{i=1}^{s_{\max}} i * |\text{CC}_i|.$$

Ranking-based strategy. The ranking strategy creates 4 rankings of the connected components in CC , finds a consensus of the rankings, and then assigns landmarks to connected components according to the consensus. Algorithm 3 illustrates the procedure. First, the algorithm creates a ranking by decreasing size (r_1), by decreasing number of vertices (r_2), by decreasing s (r_3), and by increasing number of landmarks already assigned (r_4). Then, it iteratively finds the consensus RANK via Procedure AGGRANKING and selects

a random component c^s in the first position of RANK, until the estimated oracle size Q_{est} reaches the target size Q . Similar to the sampling-based approach, Q_{est} is updated by adding $|c^s|$. Then, r_4 is updated according to the new landmark assignment. To avoid assigning more landmarks than the available hyperedges, when $|c^s|$ landmarks have been assigned to a component c^s , it is removed from all the rankings. For efficiency, the selection of the landmarks via σ is carried on iteratively, each time a new landmark is assigned to c^s (Line 10).

Procedure AGGRANKING finds the consensus by solving an instance of *Rank Aggregation with Ties*. Rank Aggregation is the task of combining multiple rankings of elements into a single consensus ranking. When the rankings are not required to be permutations of the elements, elements can be placed in the same position (*ties*). The distance between two rankings with ties π_1 and π_2 is measured as the *generalized Kendall- τ distance* $K_{\tau,p}(\pi_1, \pi_2)$ [49], which counts the pairs of elements for which the order is different in π_1 and π_2 .

The *optimal consensus* of a set of rankings $\Pi = \{\pi_1, \dots, \pi_k\}$ is the ranking π that minimizes the weighted Kemeny score (WS) [43], i.e., the weighted sum of the generalized Kendall- τ distances between π and each ranking in Π , where ω_i indicates the importance of π_i : $\text{WS}(\pi, \Pi) = \sum_{i=1}^k \omega_i \cdot K_{\tau,p}(\pi_i, \pi)$.

Several approaches have been proposed to find the optimal consensus. A recent survey [10] shows that BioConsert [14] is the best approach in many case scenarios. Since solving optimal consensus is **NP**-hard for $k \geq 4$ [8], BioConsert follows a local search approach that can result in sub-optimal solutions. The algorithm iterates over each ranking $\pi_i \in \Pi$, applies operations to π_i to make it closer to a median ranking, and finally returns the best one.

In our implementation, we assign the same importance $\alpha \in [0, 1]$ to r_1 and r_2 , and importance $\beta \in [0, 1]$ to r_3 . The importance of r_4 is set to 1, to reduce the impact of the component sizes on the consensus, hence avoiding assigning landmarks always to the same large connected components.

5.4 Landmark Selection

Given a set of landmarks L , the s -distance $\Delta_s(e, f)$ between two hyperedges e and f is upper-bounded by $\text{ub}_s(e, f) = \min_{l \in L} (\Delta_s(l, e) + \Delta_s(l, f))$. The upper bound is tight when there exists a landmark l lying on a shortest s -path between e and f : $\text{ub}_s(e, f) = \Delta_s(e, f)$. As a consequence, better ap-

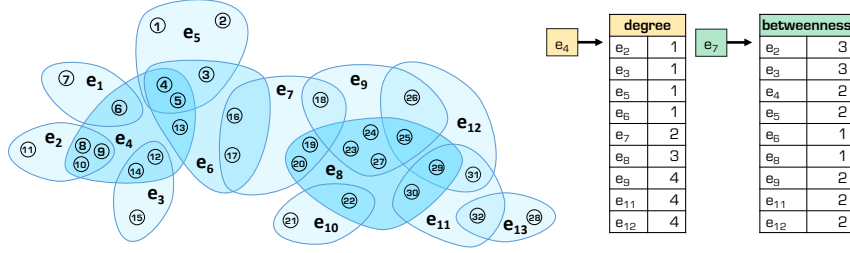


Figure 3: A hypergraph (left) and two 2-distance oracles (right) with 1 landmark selected using the **degree** (e_4) and the **BETWEENNESS** (e_7) landmark selection strategy. The oracles include the 2-distances from the landmark to all the hyperedges reachable via 2-paths.

proximations can be obtained by selecting landmarks belonging to as many shortest s -paths as possible. The optimal set of landmarks is the *2-hop s -distance cover*. A set of landmarks L is a 2-hop s -distance cover iff for any two hyperedges e and f , $\Delta_s(e, f) = \text{ub}_s(e, f)$, and L is minimal. However, finding a 2-hop distance cover is an **NP**-hard problem [59]. In the graph setting, more efficient landmark selection strategies have been proposed. Many of these can be adapted to the hypergraph setting to select landmarks within an s -connected component c^s .

Random. The **random** strategy is a baseline used to evaluate the effectiveness of the heuristics used by the more advanced strategies. It selects the landmarks uniformly at random from c^s .

Degree. Let $\Gamma_s(e)$ denote the set of s -neighbors of $e \in c^s$, i.e., the hyperedges $f \in c^s$ such that $|e \cap f| \geq s$. The cardinality of this set is called the s -degree of e . The **degree** (a.k.a. **deg**) strategy selects the hyperedges with largest s -degree.

Farthest. The **farthest** (a.k.a. **far**) strategy was originally proposed by [27] for graphs. The first landmark l_1 is selected uniformly at random from c^s . Then, iteratively, the distances from the current set of landmarks to all the reachable hyperedges are computed. The next landmark is selected from c^s such that it is the most distant hyperedge from the landmarks previously selected. Graph-based approaches usually assume graph connectivity [59]; however, as the value of s increases, the number of s -connected components in the hypergraph also increases. Therefore, it is crucial to account for this disconnectivity when implementing this strategy for the hypergraph setting.

BestCover. The **bestcover** (a.k.a. **bc**) strategy was proposed by [75] for graphs, with the goal of approximately cover as many shortest paths as

possible. In the first phase, a set of hyperedge pairs is sampled from c^s , and the shortest s -paths between them are computed. In the second phase, landmarks are iteratively chosen, such that they cover most of the shortest s -paths not yet covered by previously selected landmarks.

Betweenness. Similar to the bestcover strategy, the *between* (a.k.a. *bet*) strategy works in two phases. In the first phase, it finds all the shortest s -paths between pairs of hyperedges sampled from c^s . Then, it selects the hyperedges with highest betweenness centrality, i.e., the hyperedges that lie on most of the shortest s -paths found.

Example 3. Figure 3 illustrates a hypergraph (left) and two 2-distance oracles (right) with 1 landmark selected using the *degree* (e_4) and the *between* (e_7) landmark selection strategies, respectively. The oracles include the 2-distances from the landmark to all the hyperedges reachable via 2-paths. In this particular case, there is a giant 2-connected component consisting of all the hyperedges but e_1 , e_{10} , and e_{13} , which form separate singleton components. Therefore, each oracle stores the distances to 9 out of 13 hyperedges in the hypergraph. Note that while the 1-distance between e_7 and e_9 is 1, their 2-distance is 2, because the overlap between e_7 and e_9 is lower than 2, and thus they can reach each other only through e_8 . The *degree* oracle estimates the 2-distance between e_2 and e_6 as

$$\begin{aligned} \tilde{\Delta}_2(e_2, e_6) &= \frac{\text{lb}_2(e_2, e_6) + \text{ub}_2(e_2, e_6)}{2} = \\ &= \frac{|\Delta_2(e_4, e_2) - \Delta_2(e_4, e_6)| + \Delta_2(e_4, e_2) + \Delta_2(e_4, e_6)}{2} = 1. \end{aligned}$$

The *between* oracle estimates this distance as

$$\frac{|\Delta_2(e_7, e_2) - \Delta_2(e_7, e_6)| + \Delta_2(e_7, e_2) + \Delta_2(e_7, e_6)}{2} = 3.$$

The actual distance is $\Delta_2(e_2, e_6) = 2$.

5.5 Complexity Analysis

HYPED stores three kinds of information: the s -distance oracles, the sizes of the s -connected components, and the hyperedge-to-connected-component memberships. The space complexity is thus upper-bounded by $O(Q + s_{\max}|E| + s_{\max}|E|) = O(Q + s_{\max}|E|)$.

The running time of HYPED is determined by the time required to (i) find the s -connected components, (ii) assign the landmarks to the s -connected components, and (iii) populate the s -distance oracles. The first

step requires up to $O(s_{\max}|E| \cdot A(s_{\max}|E|^2, |E|))$, where A is the Ackermann function. The complexity of the second step depends on the landmark assignment and selection strategy used. For the ranking-based strategy equipped with **degree**, the running time is bounded by $O(s_{\max}(|E| + Q|E|^2 + L_Q|E| \log(|E|)))$; and for the sampling-based strategy equipped with **degree** is bounded by $O(s_{\max}(|E| + Q \log(|E|) + L_Q|E| \log(|E|)))$. Here L_Q is the number of landmarks selected. The third step requires up to $O(s_{\max}|E|^2)$, because, in the worst case, the number of pairs of overlapping hyperedges is $|E|^2$. Therefore the time complexity is $O(s_{\max}|E|(A(s_{\max}|E|^2, |E|) + Q|E|))$.

6 Experimental Evaluation

The experimental evaluation of HYPED has three goals. First, we discuss our design choices and the impact of each parameter on the performance of HYPED. Then, we compare the performance of HYPED with those of several baselines. Finally we showcase how HYPED can be used to **(i)** devise a recommender system, and **(ii)** approximate the closeness centrality of proteins in PPI networks.

Datasets. Table 4 reports the characteristics of all the real-world hypergraphs considered in the experimental evaluation. The data was obtained from [6, 60].^{3 4 5}

Experimental environment. HYPED is written in Java 1.8. Code and datasets are available at <https://github.com/lady-bluecopper/HYPED>. We run the experiments on a 24-Core (1.90 GHz) Intel(R) Xeon(R) E5-2420 with 126GB of RAM, Ubuntu 18.04, using all the cores available. We set $s_{\max} = 10$ and $d_{\min} = 4$ for all experiments. For convenience, we set $Q = \ell \cdot |E|$, and pass the parameter ℓ to Algorithm 1 instead of Q . As HYPED involves a probabilistic component, we execute each experiment 10 times with different seeds and report averages. Finally, the query hyperedges are randomly selected via a stratified sampling algorithm, which ensures that the set of queries includes hyperedges connected via s -paths for $s \in [1, 10]$. Recall that the higher s , the lower the probability that two hyperedges are in the same s -connected component. Hence, a naive sampler might select too few hyperedges connected via higher-order paths.

Metrics. We evaluate the performance of the algorithms according to four metrics. The lower their value, the better the algorithm. **OFF** indicates

³<http://www.sociopatterns.org/datasets>

⁴<http://konect.cc/networks>

⁵<https://snap.stanford.edu/biodata>

Table 4: Characteristics of the datasets: number of nodes, number of hyperedges, maximum size of a hyperedge, number of hyperedges of size greater than 2, and number of hyperedges of size greater than 3.

Dataset	$ V $	$ E $	d	$ E_2 $	$ E_3 $
NDC-C	1.1K	1K	24	1K	750
ETFs	2.3K	2K	19	1.6K	985
High	327	8K	5	7.8K	2.3K
Zebra	10K	10K	62	4.9K	3.7K
NDC-S	5.3K	10K	25	6.3K	5.1K
Primary	242	13K	5	12 704	4956
Enron	50K	106K	64	104K	68K
Epinions	756K	107K	162K	73K	60K
IMDB	1M	267K	10	257K	245K
DBLP	1.9M	2.4M	17	2.2M	1.5M
Threads-SO	2.7M	7M	22	5.2M	1.3M
chem-gene	2.3K	2.5K	147	1.7K	1.2K
dis-function	16K	3.4K	6.3K	3.4K	3.4K
dis-gene	17K	3.9K	6.2K	2.2K	2K
dis-chemical	1.7K	4.7K	1.1K	4.4K	4.2K

the time required to create the data structures (e.g., indices or oracles) used at query time; **TimeXQ** is the average time required to answer a distance query; **MAE** is the mean absolute error of the distance estimates; **RMSE** is the root mean squared error of the distance estimates. Furthermore, in some analyses, we show the distribution of the L_1 -norm of the differences between real distances and estimates.

We note that accuracy bounds of distance oracles have been proven only for connected graphs [5]. For disconnected graphs, they are hard to obtain, unless some connectivity assumption is made. For this reason, we evaluate the accuracy of HYPED only empirically.

Baselines. We compare two versions of Algorithm 1 (HYPED and HYPED-IS) with (i) an approximate baseline, BASELINE, designed for hypergraphs, and (ii) two state-of-the-art approaches, CTL [52] and HL [19], designed for graphs. We do not consider the method presented in [61], as it is a distributed algorithm, while we focus on centralized algorithms. The hypergraph-oriented algorithms are implemented in Java 1.8, while the graph-oriented algorithms are written in C++11.

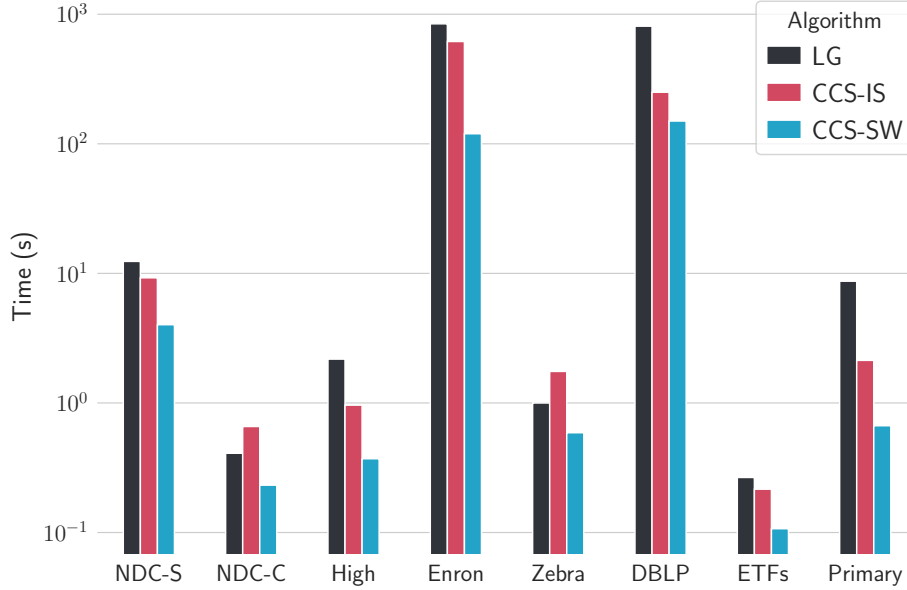


Figure 4: Time required to find the s -connected components for $s \in [1, 10]$ using LG, CCS-IS, and CCS-SW.

Table 5: Comparison between **Sampling** and **RankAgg**: MAE, RMSE, oracle building time (OFF), and (average) number of landmark assigned (NL).

Dataset	RankAgg				Sampling			
	MAE	RMSE	OFF (s)	NL	MAE	RMSE	OFF (s)	AVG NL
ETFs	0.5980	1.5490	16.400	1281	0.7489	1.6201	2.170	356.9
High	0.9411	1.5703	14.537	545	1.2167	1.8691	11.971	103.6
NDC-C	0.4442	0.8564	2.856	309	0.5150	0.8972	1.444	147.5
NDC-S	0.7019	1.1286	103.830	1559	0.8732	1.2312	38.706	195.0
Primary	0.7881	1.1833	48.861	649	0.9973	1.3118	39.560	108.6
Zebra	1.3288	2.4162	95.767	2328	1.6445	2.3963	4.850	377.5

HYPED, HYPED-IS, and BASELINE create an s -distance oracle for each s up to s_{\max} , but they differ in how they populate them. BASELINE assigns landmarks with no regard to the connectivity of the hypergraph at the different values of s . Given a target oracle size Q and an estimated oracle size Q_{est} initialized to 0, it iterates until $Q_{\text{est}} \geq Q$. At each iteration, it assigns $(Q - Q_{\text{est}})/(|E| * s_{\max})$ landmarks to each s -distance oracle, according to

one of the landmark selection strategies. HYPED-IS assigns the landmarks to each s -distance oracle independently, while exploiting the information on the s -connected components. Given a target oracle size Q , it ensures that each s -distance oracle has size Q/s_{\max} , by calling Procedure SELECTLANDMARKS with inputs $CCS = s$ -connected components, and Q/s_{\max} in place of Q . This algorithm differs from HYPED in that it treats all the oracles equally, and finds the s -connected components by using CCS-IS. Since all the connected components given to the probabilistic strategy are s -connected components for the same value of s , β is set to 0. Finally, HYPED is simply Algorithm 1.

CTL [52] improves the state-of-the-art 2-hop pruned landmark labeling approach (PLL [2]), by first decomposing the input graph in a large *core* and a *forest* of smaller trees, and then constructing two different indices on the core-tree structure previously generated. A parameter d bounds the size of the trees in the forest and regulates the trade-off between index size and query time. We denote the algorithm with CTL- d .

HL [19] is a landmark-based algorithm that first selects a set of l vertices, and then populates a *highway* and a *distance* index. At query time, the algorithm first finds an upper-bound to the distance exploiting the highway index, and then, finds the distance in a sparsified version of the original graph. We denote the algorithm with HL- l .

6.1 Performance Analysis of HypED

We first compare the algorithm for computing the s -connected components against two baselines. Then, we discuss the differences between the two procedures to assign landmarks.

Connected Components. We compare Algorithm 2 with two non-trivial baselines. All the three strategies are based on the union-find algorithm, but they differ in how they exploit it. The first baseline (LG) constructs the line graph $\mathcal{L}(H)$ by iterating over the hyperedges, exploiting a dynamic inverted index to efficiently find the number of vertices that each hyperedge shares with the other hyperedges. Then, it runs union-find for each s -line graph \mathcal{L}_s . The second baseline, CCS-IS (*Independent Stages*), finds the s -connected components for each s separately. Each time, it builds a dynamic inverted index to find the hyperedge s -overlaps, and then runs union-find using those overlaps.

Figure 4 shows the running time of the algorithms on all the datasets, for $s \in [1, 10]$. In most cases, the line-graph-based is the most expensive, as it must compute all the pairwise hyperedge overlaps. Our technique, that in

Figure 4 is dubbed CCS-SW, (*StageWise*), outperforms the two baselines in all the datasets, thanks to the exploitation of (i) the $(s + 1)$ -connected components for the initialization of the s -connected components, and (ii) the transitive property for the reduction of the number of overlaps to compute.

Landmark assignment strategies. In the following experiments, we set $\ell = 30$ and select the landmarks using the **degree**, the **farthest**, and the **bestcover** selection strategy. For the sampling-based strategy (**Sampling**), we consider the values $\{0.2, 0.33, 0.4\}$ for α and $\{0.6, 0.33, 0.2\}$ for β . We pick such values with the goal of comparing the performance of HYPED when (i) there is a higher probability of assigning a landmark to a higher-order connected component ($\alpha < \beta$), (ii) there is a higher probability of assigning a landmark to a larger connected component ($\alpha > \beta$), and (iii) the contribution of the component size and of s is the same ($\alpha = \beta$). We note that any other combination of values can be used as well, as long as $2 \cdot \alpha + \beta = 1$.

Figure 5 shows that we can achieve more accurate estimates by giving more importance to the value of the parameter s , rather than the component size. Indeed, higher values of α increase the probability of selecting landmarks within the same connected components (the largest ones), whereas larger values of β increase the probability of selecting connected components of various sizes. In fact, the latter configuration ensures the selection of landmarks in s -connected components for different values of s . In turn, selecting landmarks in different s -connected components allows the oracle to answer a wider number s -distance queries, because at least one landmark is needed to obtain lower and upper bounds to the actual distance. The answers, however, may be less accurate. By looking at the mean MAE values, we observe lower errors when using the parameter combination $(\alpha, \beta) = (0.2, 0.6)$.

For the ranking-based strategy (**RankAgg**), we considered the values $\{0.5, 0.8, 1.0\}$ for both α and β . When α is 1, we observe worse MAE values (Figure 6), because the probability of selecting landmarks in different connected components is higher when the importance factor of r_4 is strictly higher than the other factors. In all other cases, differently from the sampling-based strategy, the performance are comparable, which means that the MAE values for the combinations $\alpha \leq \beta$ and $\alpha \geq \beta$ are nearly identical. By looking at the oracle building times, we select the combination $(\alpha, \beta) = (0.5, 0.5)$ as best performing combination.

Table 5 reports a comparison between the sampling-based strategy with $(\alpha, \beta) = (0.2, 0.6)$ and the ranking-based strategy with $(\alpha, \beta) = (0.5, 0.5)$, which are the best performing variants of the two strategies. It shows MAE,

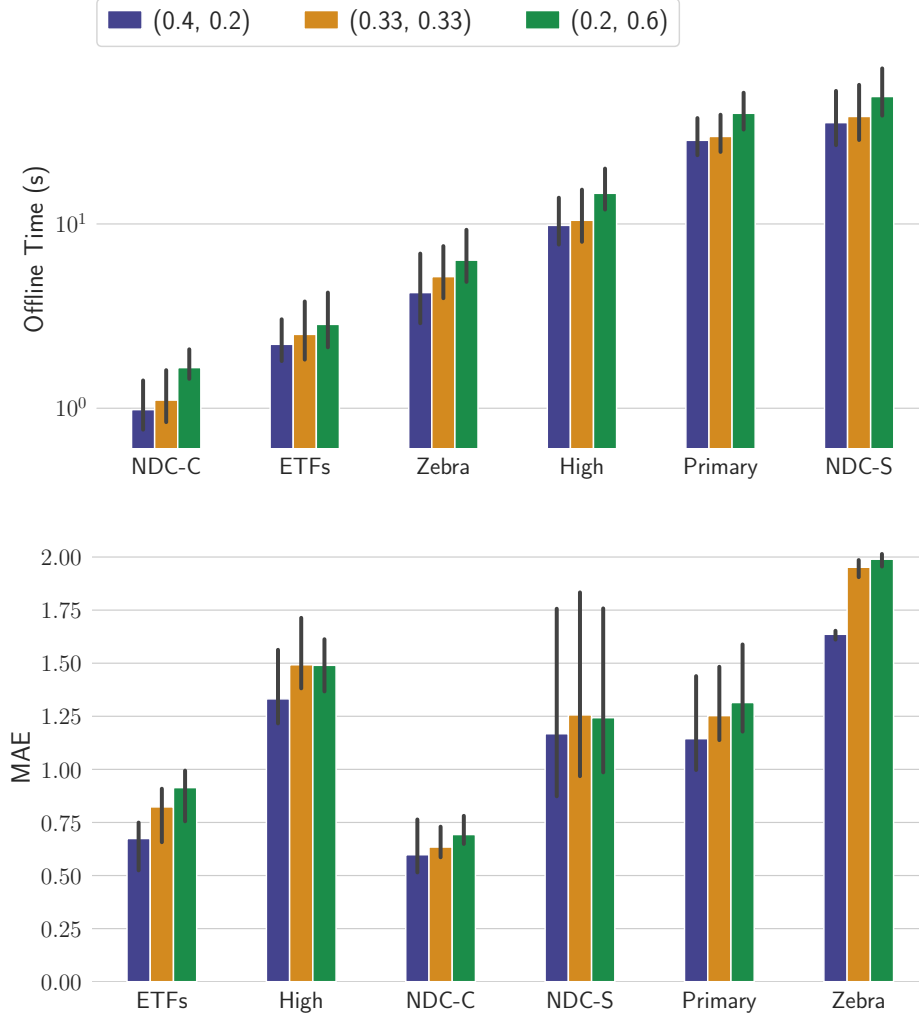


Figure 5: Oracle building time (top) and MAE (bottom) using the **Sampling** landmark assignment strategy for different combinations of importance factors (α, β) . The charts report mean and standard deviation among the values for the **degree**, **farthest**, and **bestcover** landmark selection strategies.

RMSE, OFF, and number of landmarks assigned, for several datasets.

Due to the high time complexity of BioConsert, **RankAgg** shows worse running time than **Sampling**. Whereas the running time of **Sampling** is affected by the hypergraph size and the number of connected components,

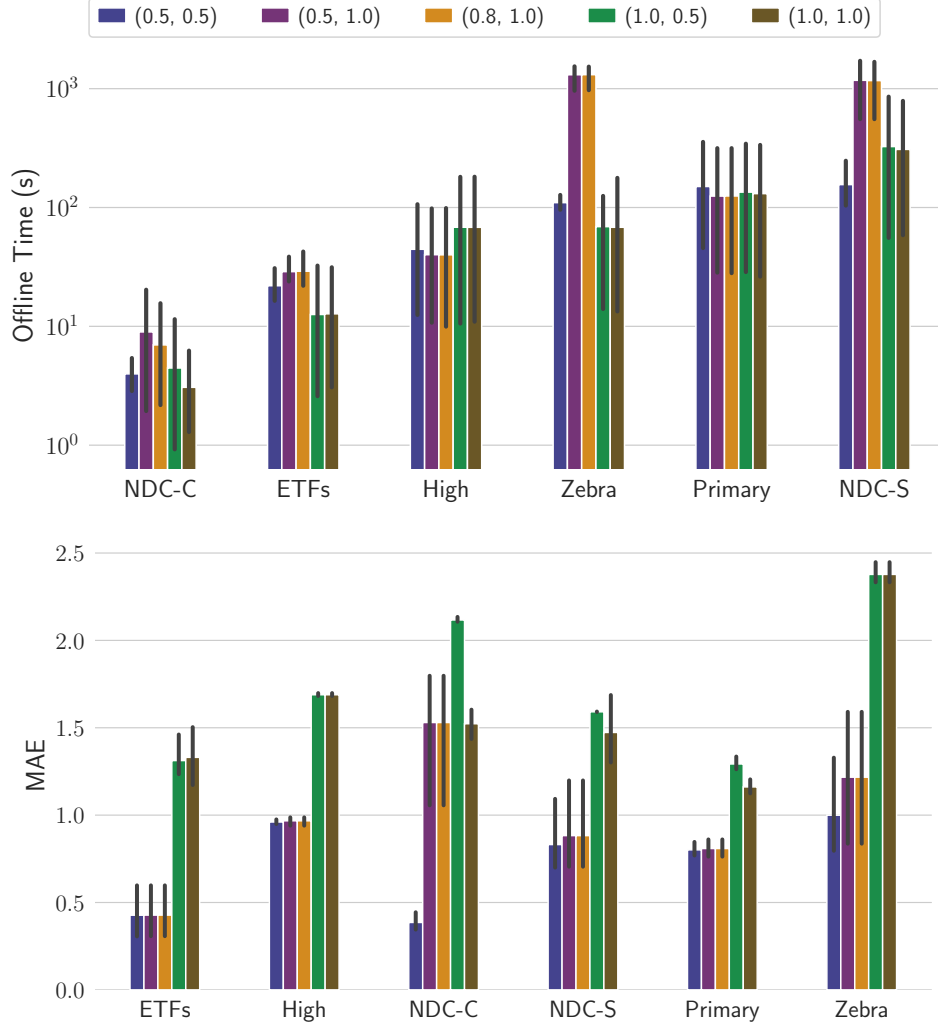


Figure 6: Oracle building time (top) and MAE (bottom) using the Rank-Agg landmark assignment strategy for different combinations of importance factors (α, β) . The charts report mean and standard deviation among the values for the **degree**, **farthest**, and **bestcover** landmark selection strategies.

that of RankAgg depends also on its past choices: each landmark assignment changes r_4 , which, in turn, can complicate the task of finding a consensus. This higher complexity comes with better results, though. The MAE and RMSE consistently remain lower than those of Sampling, except for the RMSE in Zebra. Indeed, RankAgg distributes the landmarks more uniformly

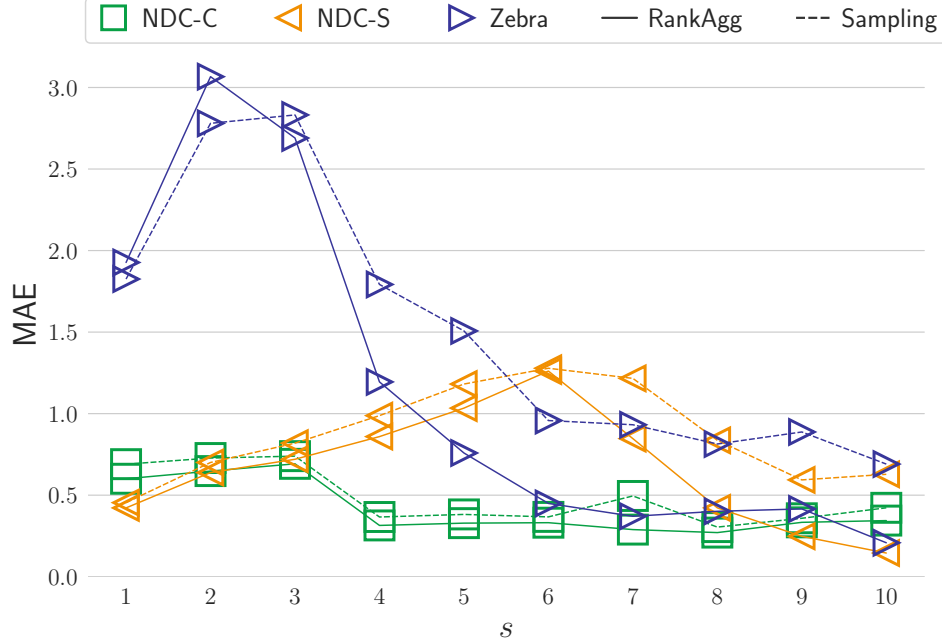


Figure 7: MAE of s -distance queries for different values of s , using the Sampling and the RankAgg landmark assignment strategy and the degree landmark selection.

across the connected components and, in particular, assigns them to smaller connected components. As a result, given a budget Q , it can assign more landmarks, and hence cover more connected components than **Sampling**. In the case of the largest connected components, typically found at smaller values of s , both strategies converge to a similar number of landmark assigned. This similarity results in similar approximate distance computations. Consequently, the MAE curves in Figure 7 behave similarly for smaller s values. However, a noticeable distinction emerges at larger s values, because the corresponding s -connected components are smaller and thus better covered by RankAgg.

Landmark selection strategies. We evaluate the performance of our algorithm when varying the landmark selection strategy. We keep all the other parameters fixed: $\ell = 30$, $\alpha = 0.2$ and $\beta = 0.6$ for **Sampling**, and $\alpha = \beta = 0.5$ for RankAgg. For **bestcover** and **between**, we sample 40% of the hyperedges to find the shortest paths.

Figure 8 illustrates the OFF time for **Sampling** (top) and for RankAgg

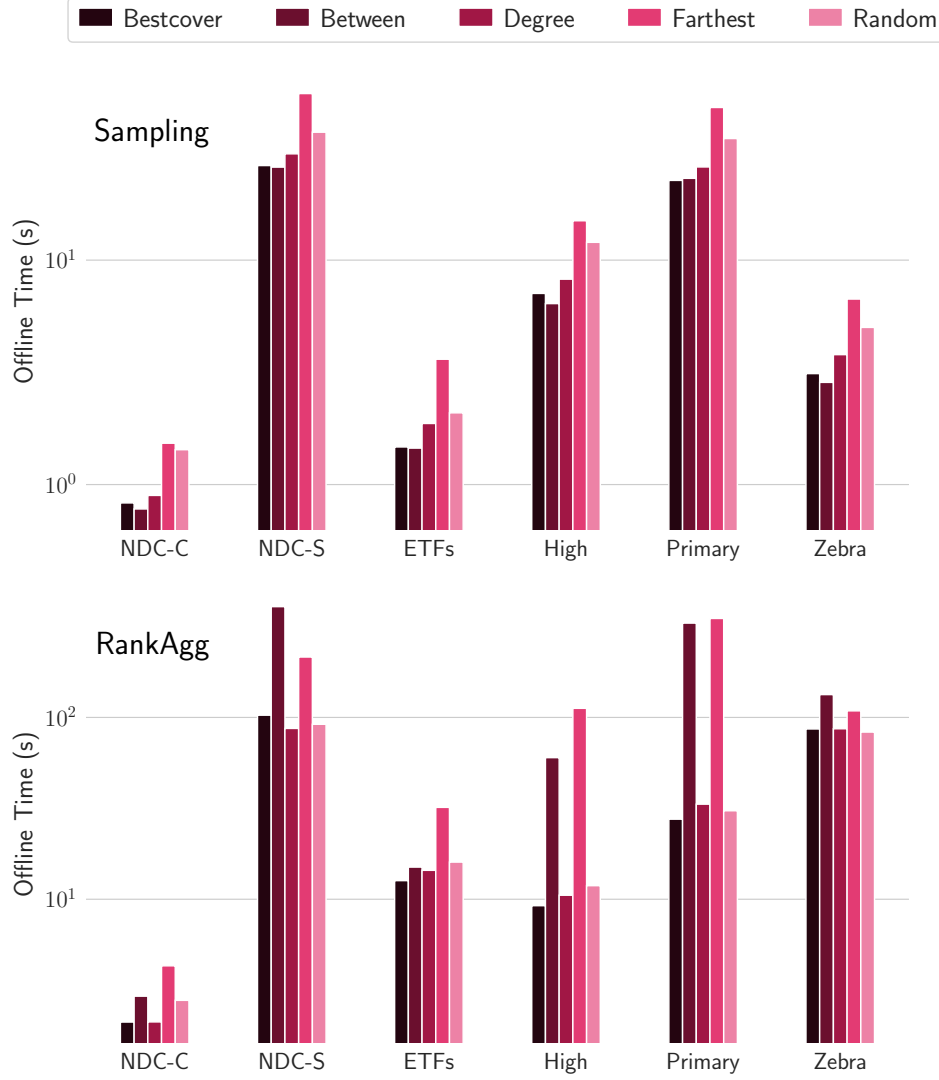


Figure 8: Time required to create the distance oracle when using the Sampling (top) and the RankAgg landmark assignment strategy and different landmark selection strategies.

(bottom), while Figure 9 displays the corresponding MAE values, for several datasets. For Sampling, the running time is comparable, with random and farthest being the slowest. The running time of the former is affected by the poor selection of the landmarks (the population of the oracle for pe-

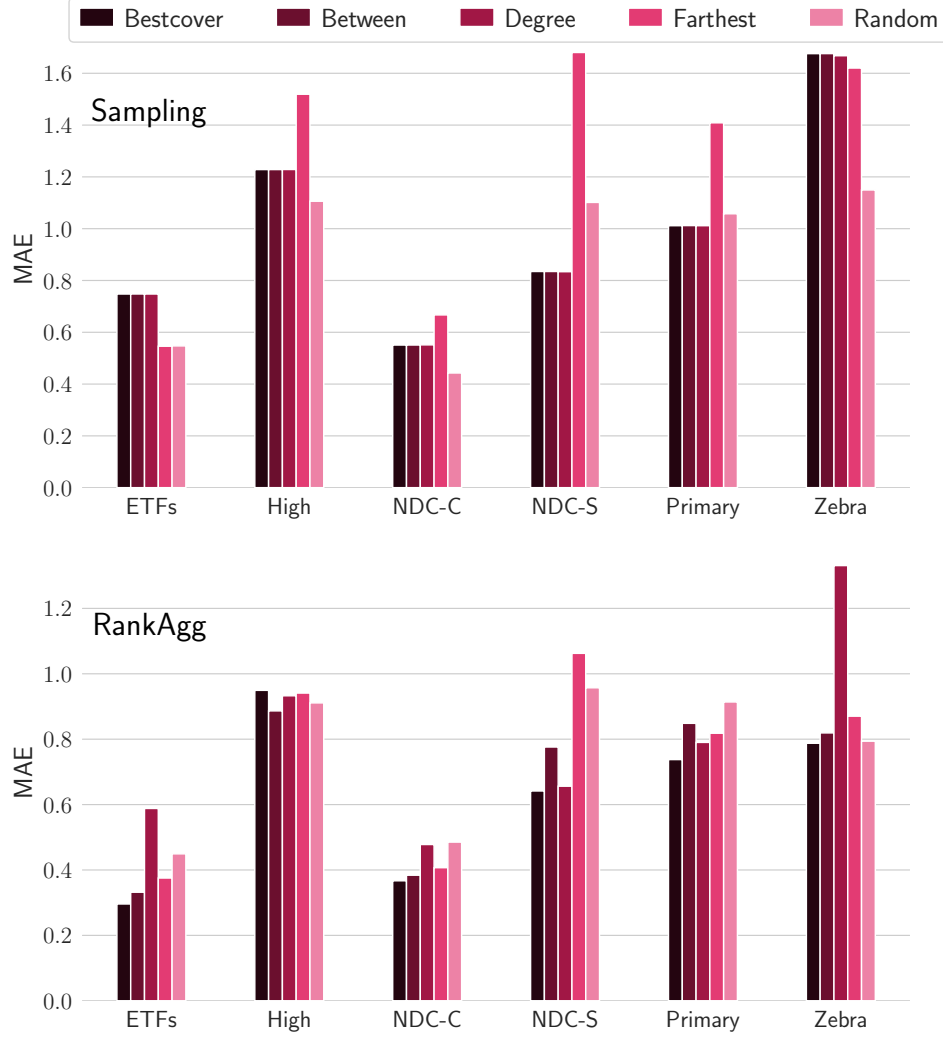


Figure 9: MAE values when using the Sampling (top) and the RankAgg landmark assignment strategy and different landmark selection strategies.

ripheral landmarks takes more time than that for central landmarks), while that of the latter is further increased by the procedure used to find all the hyperedges reachable from the landmarks already selected. In the case of RankAgg, we observe a significantly higher running time also for between. This outcome can be attributed to RankAgg’s tendency towards selecting a larger number of landmarks and to the higher complexity of between to se-

Table 6: MAE, RMSE, average query time, and average creation time, for BASELINE, HYPED-IS, and HYPED.

Dataset	BASELINE			
	MAE	RMSE	TimeXQ (μ s)	OFF (s)
ETFs	1.6635	2.3319	0.882	2.4064
High	1.5602	2.0992	0.947	10.1148
NDC-C	1.1095	1.6988	0.482	1.1090
NDC-S	1.3864	1.7209	0.436	54.2579
Primary	1.3616	1.7490	0.887	35.2953
Zebra	2.4091	2.7392	0.439	6.5455

Dataset	HYPED-IS			
	MAE	RMSE	TimeXQ (μ s)	OFF (s)
ETFs	1.0893	2.1026	0.387	0.4399
High	1.1822	1.9806	0.691	3.0960
NDC-C	0.5924	0.9937	0.422	1.0896
NDC-S	0.8162	1.2194	0.425	33.8278
Primary	0.8985	1.3510	0.677	10.2065
Zebra	1.6687	2.5321	0.501	4.7281

Dataset	HYPED			
	MAE	RMSE	TimeXQ (μ s)	OFF (s)
ETFs	0.7437	1.6185	0.769	1.5461
High	1.2167	1.8691	0.745	8.2114
NDC-C	0.5150	0.8972	0.408	0.8031
NDC-S	0.8732	1.2312	0.328	25.7270
Primary	0.9973	1.3118	0.685	26.0442
Zebra	1.6427	2.3959	0.374	4.2102

lect a landmark. By looking at the MAE, we can observe that, as expected, **bestcover** and **between** have similar performance, and are more frequently among the top-3 selection strategies. Surprisingly, **random** reaches the top-3 in 4 out of 6 datasets for **Sampling**, proving the hardness of the landmark selection task in the case of very disconnected hypergraphs.

Since the difference in performance is relatively small and the running time of **Sampling** is more predictable AND UP TO AN ORDER OF MAGNITUDE LOWER THAN THAT OF **RANKAGG**, the following experiments use **Sampling** as landmark assignment strategy.

Desired oracle size and d_{\min} . We investigate the influence of ℓ and d_{\min} on both the size and accuracy of the oracle in s -distance approxima-

tions. To this aim, we vary ℓ in $[100, \dots, 600]$ and d_{\min} in $[3, 4, 6, 12]$. We use the **Sampling** landmark assignment strategy with $\alpha = 0.2$ and $\beta = 0.6$ and the **degree** landmark selection strategy. Figure 10 and Figure 11 illustrate the oracle sizes (in MB), the oracle building time (s), and the MAE for four datasets: NDC-C, Zebra, ETFs, and High. We observe that d_{\min} has minimal impact on the oracle size, as it essentially determines which s -connected components must be stored in the oracle and this information does not affect significantly the total size. Similarly, it exerts little influence on the building time, serving mainly as a filter for connected components considered during the landmark assignment step. However, there is a subtle effect on the MAE values. Allowing the assignment of landmarks to components of sizes 5 and 6 results in more accurate answers to a larger number of distance queries, consequently leading to lower MAE values.

As expected, the oracle size grows linearly with ℓ . This growth, however, comes with an exponential surge in the running time. In fact, each additional inclusion of a landmark requires the computation of all the distances from this landmark to every other hyperedge within the same s -connected component, a number that can escalate up to $|E_s|$ hyperedges. In contrast, the improvement in MAE has a slow rise, with a significant inflection point around $\ell = 200$. Across most datasets, we note low MAE values at $\ell = 400$, suggesting a favorable trade-off between accuracy and computation time.

6.2 Comparison with Baseline

We first present the comparison among HYPED, HYPED-IS, and BASELINE. Table 6 and Figure 12 report the metrics for $\ell = 30$ and the degree landmark selection strategy. The figure displays the results only for the dataset Zebra, but we observe similar behaviors in all the other datasets. BASELINE displays a higher OFF time, as it needs to perform several iterations before using up all the budget. Conversely, HYPED-IS and HYPED have roughly the same creation time: HYPED-IS takes more time to find the s -connected components, whereas the landmark assignment process of HYPED is more complex. While they tend to assign a similar number of landmarks, these algorithms differ in *where* they assign them: HYPED assigns roughly the same number of landmarks to each s -distance oracle, whereas HYPED-IS assigns more landmarks to higher-order distance oracles. This effect is a result of HYPED-IS splitting the budget evenly among the s -distance oracles, and, at higher values of s , the hypergraph is more disconnected; thus, each landmark has a lower cost on the budget. Similar to HYPED, BASELINE assigns the landmarks evenly among the s -distance oracles, but it fulfills the

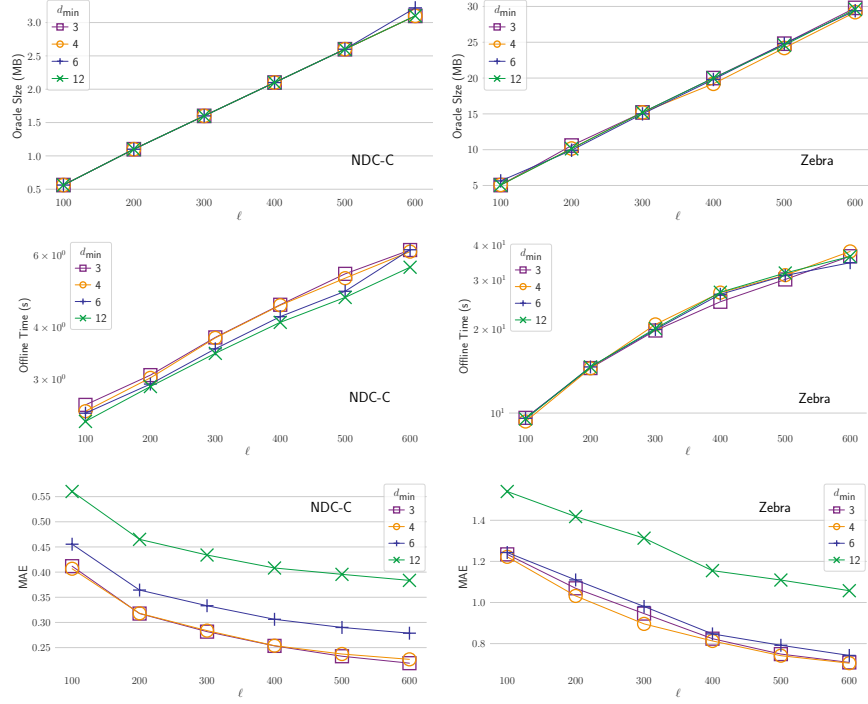


Figure 10: Oracle size (MB, top), oracle building time (s, middle), and MAE (bottom) for NDC-C (left) and Zebra (right), varying ℓ and d_{\min} , using the **Sampling** landmark assignment strategy and the **degree** landmark selection strategy.

budget by using a lower number of landmarks, because it tends to assign landmarks to larger connected components.

Regarding the average query time, since BASELINE is not aware of the connectivity of the hypergraph at various s , it takes more time to answer queries involving hyperedges either not connected or in the same small connected component. As a consequence its TimeXQ is higher. In contrast, HYPED-IS and HYPED exploit the information on the s -connected components to assign the landmarks strategically, and hence they achieve both a lower TimeXQ and a lower MAE. Even though HYPED and HYPED-IS display comparable MAEs in most of the datasets considered, we note that HYPED is more versatile, because it always fully exploit the budget available. In contrast, HYPED-IS may construct oracles with size far lower than the desired value, due to the hypergraph being highly disconnected at larger

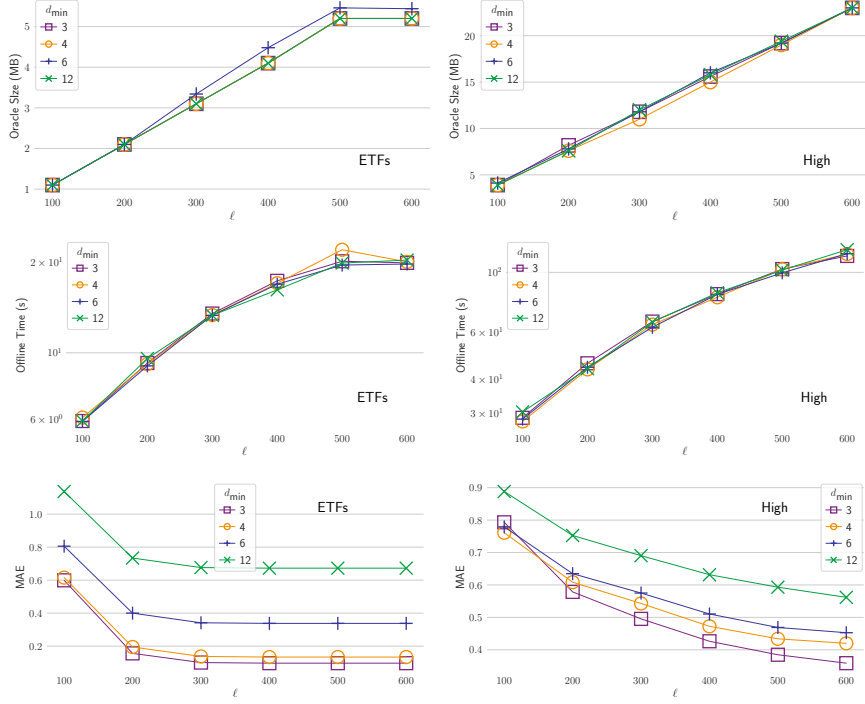


Figure 11: Oracle size (MB, top), oracle building time (s, middle), and MAE (bottom) for ETFs (left) and High (right), varying ℓ and d_{\min} , using the Sampling landmark assignment strategy and the degree landmark selection strategy.

values of s . This is a consequence of the fact that HYPED-IS divides the budget equally among the various s -distance oracles, before computing the s -connected components for each value of s .

6.3 Comparison with line-graph-based Oracles

We build line-graph-based oracles (Section 4) via two state-of-the-art exact oracles for graphs, CTL [52] and HL [19] on top of the line graph. Note that HL and CTL are exact only for connected graphs: HL exploits this property in the construction of the highway labeling index, while CTL exploits it in determining core and peripheral nodes. As a consequence, when the graph is not connected (as often happens in our setting for larger values of s), they may introduce errors.

We recall that no existing work can simultaneously answer the three

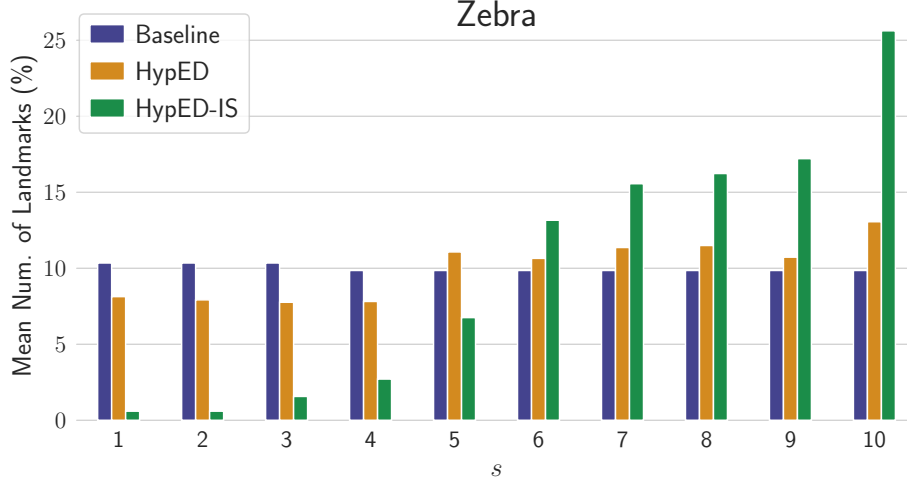


Figure 12: Mean number of landmarks selected by BASELINE, HYPED-IS, and HYPED, for each s -distance oracle, in Zebra.

types of s -distance queries considered in this work, nor build distance profiles as defined in Problem 1. Thus, we compare our framework against HL and CTL, only in the task of hyperedge-to-hyperedge s -distance query answering, for s up to 10. To this aim, we sampled 100 pairs of hyperedges 5 times (for a total of 500 queries for each s), ensuring that (i) most of the pairs are connected for each s , (ii) all pairs are 1-connected, and (iii) most of the pairs belong to (the same) large connected components. This way, we guarantee that a substantial amount of queries has a finite answer.

Figure 13 illustrates the metrics of CTL, HL, and our algorithm. The OFF time of CTL and HL includes the time required to find the line graph of the hypergraph. We report the running times of CTL and HL for completeness, even though they are not fairly comparable with those of our algorithm because they are written in C++. We do not show results for CTL in Threads-SO because the algorithm runs out of memory and is not able to complete.

OFF. For CTL and HL we present the creation times with respect to only one parameter combination, because the index creation time is determined principally by the time required to find the line graph. Hence the total creation time changes only slightly with the parameters of the algorithms, d and l .

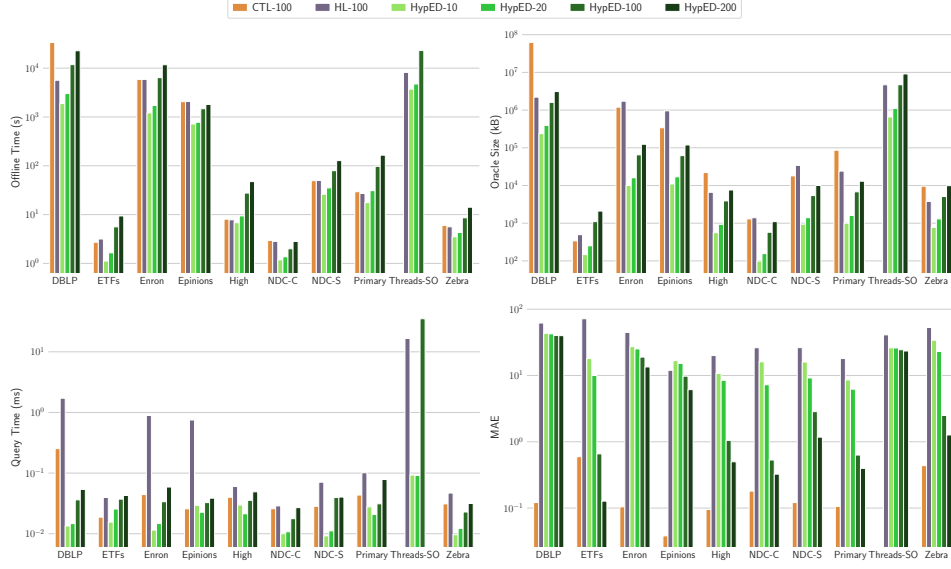


Figure 13: OFF time (upper left), oracle disk size (upper right), TimeXQ (lower left), and MAE (lower right) of CTL, HL, and our algorithm varying ℓ (HYPED- ℓ) and fixing **degree** as landmark selection strategy, **Sampling** as landmark assignment strategy, $\alpha = 0.2$, $\beta = 0.6$, and $d_{\min} = 4$.

Instead, we assess the scalability of HYPED by varying the parameter ℓ . Note that the time required to populate the landmark-based distance oracle depends on several factors: hypergraph size, hypergraph dimension, and hyperedge overlap. As an example, even though Primary is larger than NDC-S, the running times are comparable because the dimension of NDC-S is larger. Similarly, IMDB has twice as many hyperedges as Enron and Epinions, but its dimensionality is less than $1/6$ of theirs. In addition, the average number of hyperedges to which a node belongs is only 2 in IMDB, but grows to 7.16 and 18 in Enron and Epinions. The larger this number, the more the hyperedges overlap, and thus the more complex the tasks of finding connected components and shortest paths. The complex behavior of the algorithm is more evident in DBLP. This dataset is one order of magnitude larger than Enron, but the running time is not significantly higher. This result is again due to the lower dimensionality and average node occurrence of the former dataset.

Oracle size. Especially for larger hypergraphs, the size required to store the CTL index is much larger than that of storing the landmarks-based oracle.

As an example, the CTL index for DBLP takes up to 93GB ($d = 10$), while HYPED takes up to 3.1GB ($\ell = 200$). Note that there is little to no control over the index size of CTL, while the index size of HYPED can be decided by the user according to their needs. The size of CTL does not change much with d , as the tree-index size is proportional to d and the core-index size is inversely proportional to d . Instead, the index size of HL increases linearly with l , but its total disk size is dominated by the size of the graph, which is required at runtime to compute the distances.

TimeXQ. We evaluate the time required to answer distance queries for 100 pairs of hyperedges, selected with a stratified sampler that ensures a fair amount of finite s -distances for each $s \in [1, 10]$. We repeat the test 3 times and report the average query time.

The TimeXQ of CTL and HYPED is usually lower than that of HL, with HYPED achieving the lowest query times on the largest datasets (DBLP and Enron). The query time of HYPED grows with ℓ (more landmarks means more candidate lower and upper bound to consider to get the final estimate), while the query time of CTL and HL remains relatively stable when increasing d and l . For CTL, this result stems from the amount of information stored in the index being basically constant; while for HL, from the query time being dominated by the time required to evaluate the queries on the sparsified version of the graph.

MAE. CTL and HL are exact algorithms designed for connected graphs. As a consequence, in disconnected graphs such as s-line graphs, they are not guaranteed to provide exact answers. Nevertheless, thanks to a more substantial index, CTL displays lower MAE values, with higher errors in ETFs and Zebra (despite them being neither the largest nor the most disconnected graphs). In contrast, HL, with an index size comparable to that of HYPED-200, has the worst performance in all the datasets.

For the largest datasets, there is no significant improvement when increasing ℓ for HYPED. Indeed, the number of additional landmarks introduced, and hence additional distance pairs stored, is relatively small compared to the total number of hyperedges. Thus, the probability of a landmark being on a shortest path between two query hyperedges does not increase much.

Discussion. We reported a comparison on hyperedge-to-hyperedge queries between line-graph-based oracles (Section 4), by using two state-of-the-art methods for connected graphs, and the landmark-based HYPED framework (Section 5). We cannot compare on vertex-to-vertex and vertex-to-hyperedge queries, because CTL and HL are not designed to work on the

augmented line graph. In particular, since they lack the ability to distinguish nodes representing vertices from nodes representing hyperedges, they cannot ensure to (i) perform BFSs traversing only hyperedges, and (ii) to select only hyperedges as landmarks. In the experiments on larger datasets, HYPED allows the creation of indices far smaller than those created by CTL on the line graph, while guaranteeing a small TimeXQ, and MAE comparable with HL. As an example, the CTL index size for DBLP is 93GB, whereas our oracle size is 3.1GB. In addition, we remark that CTL failed to generate an index for the largest dataset, due to memory issues. We also remark that the query times of CTL and our oracle may not be directly comparable, primarily due to the fact that CTL is implemented in C++ while our algorithm is in Java. As discussed in Section 4, the limits of line-graph-based oracles emerge with larger hypergraphs, where the line graph size and creation time depend on the characteristics of the hypergraph, and thus can not be controlled. Instead, the landmark-based HYPED framework allows fine-grained control of the trade-off between index size and approximation error at creation time.

Finally, we highlight that while HL requires access to the input hypergraph to answer the distance queries, HYPED does not. This characteristic can be advantageous in scenarios where end-users are granted limited access to the original data and are restricted to interacting solely with the oracle. Nevertheless, in instances where the original hypergraph is accessible, HYPED can be adapted to incorporate this information, with the advantage of being able to calculate the exact s -distances for pairs of hyperedges within the same small s -connected components through bidirectional BFS. This would be, however, at the price of higher query times.

6.4 Hypergraph-based Recommendations

Collaborative filtering recommender systems typically model users as sets of items they liked and each item as the set of users it is liked by. Hypergraphs, going beyond the binary relations, allows to model relations among sets, paving the way for higher-order recommender systems capable of fully leveraging the available information. The integration of higher-order distance oracles can enhance existing random-walk-based methods [30, 16, 31] designed to assign scores to items that may be of interest to a user. For instance, if the hypergraph models a user’s in-session listened songs, we can recommend a new playlist comprising diverse yet related songs based on the user’s previous listening session. In contrast, representing the data as a graph loses the information about which songs were listened to together by

Table 7: Avg precision ($\ell = 70$) in finding the top- k closest elements with the same label of the query.

s	AveP@3		AveP@7	
	IMDB	DBLP	IMDB	DBLP
2	0.699	0.587	0.760	0.619
3	0.886	0.812	0.916	0.812
4	0.967	0.927	0.980	0.927
5	0.988	1.000	0.995	1.000
6	0.993	1.000	0.996	1.000
7	0.997	1.000	1.000	1.000
8	1.000	1.000	1.000	1.000
9	1.000	1.000	1.000	1.000
10	1.000	1.000	1.000	1.000

the user.

Following [59], in this section, we show how s -distance oracles can be embedded into a hypergraph-based recommender system. One of the advantages of such type of recommender system is that, by using higher values of s , we can tune the strength of the relations behind the recommendations given. We consider two labeled hypergraphs: IMDB and DBLP. In IMDB, each hyperedge represents a movie and each vertex is a member of its crew. Vertices are associated with a label indicating their role in the movie (e.g., actor, actress, producer, director). In DBLP, each hyperedge represents a scientific publication and each vertex is an author. Hyperedges are associated with a label that indicates the venue where the article was published. The idea is to recommend the k -nearest neighbors among the elements which have the same label. That is, in IMDB we recommend other individuals who have covered the same role of the query vertex and have participated in movies that are close to the ones of the query vertex. In DBLP, given an article (a hyperedge), we recommend other articles which have been published in the same venue and are close to the query hyperedge in terms of co-authors. We use HYPED to quickly approximate s -distances: in the case of IMDB, the oracle answers vertex-to-vertex distance queries, while in the case of DBLP, it answers hyperedge-to-hyperedge distance queries. As queries, we select 5 labels at random, then we sample vertices or hyperedges with one of those labels. For comparison, we also compute the exact k -nearest neighbors, via BFS.

Precision@k. Table 7 reports the average precision in the computation of the top-3 and top-7 closest elements to the query, varying s . With such a small oracle size, the MAE of HYPED is 0.90 in DBLP, and 1.44 in IMDB.

Table 8: Top-5 suggestions provided by HYPED for a query article, for two values of the parameter s .

Query: <i>Incorporating Pre-Training in Long Short-Term Memory Networks for Tweets Classification.</i>
Top-5 Suggestions ($s = 1$)
Personalized Grade Prediction: A Data Mining Approach
Predicting Sports Scoring Dynamics with Restoration and Anti-Persistence
R2FP: Rich and Robust Feature Pooling for Mining Visual Data
Mining Indecisiveness in Customer Behaviors
New Probabilistic Multi-graph Decomposition Model to Identify Consistent Human Brain Network Modules
Top-5 Suggestions ($s = 2$)
R2FP: Rich and Robust Feature Pooling for Mining Visual Data
New Probabilistic Multi-graph Decomposition Model to Identify Consistent Human Brain Network Modules
KnowSim: A Document Similarity Measure on Structured Heterogeneous Information Networks
Leveraging Implicit Relative Labeling-Importance Information for Effective Multi-label Learning
Generative Models for Mining Latent Aspects and Their Ratings from Short Reviews

Nevertheless, we can see that for $s \geq 3$ the average precision is close to optimal, i.e., the rankings provided by HYPED are almost identical to the exact ones while being produced in a fraction of the time required by an exact k -nearest neighbors computation.

Anecdotal Evidence. Table 8 shows an example of the top-5 suggestions for a query (an article) in DBLP, for two values of s . The query considered is the article ‘*Incorporating Pre-Training in Long Short-Term Memory Networks for Tweets Classification*’. The fields of research of the authors are data mining, machine learning, and deep learning. Different values of s bring different sets of recommendations and different rankings. In particular, the article ‘*Predicting Sports Scoring Dynamics with Restoration and Anti-Persistence*’ takes the second position in the rank by 1-distance, but its 2-distance from the query is so large that it is not included in the rank by 2-distance. This result indicates that the two articles are weakly related, as it can be gathered by examining the topics they address. The two articles ‘*R2FP: Rich and Robust Feature Pooling for Mining Visual Data*’ and ‘*New Probabilistic Multi-graph Decomposition Model to Identify Consistent Human Brain Network Modules*’ are included in both rankings, but the second article is in a higher position in the rank by 2-distance. Clearly, the article is farther from the query, but its connection is stronger. Finally, by looking at the topics studied in the query and in the suggestions per ranking, we can see that the article ‘*KnowSim: A Document Similarity Measure on Structured Heterogeneous Information Networks*’ overlaps more with the query, and hence it may be more interesting for the user. In fact, the query article proposes a deep learning algorithm that learns dependencies between words in tweets to solve a tweet classification task, while KnowSim builds heteroge-

neous information networks to identify similar documents (e.g., tweets), and hence can effectively classify documents into any desired number of classes.

As another example, in IMDB, given as query the producer Barry Mendel, our method suggests the producer Yuet-Jan Hui (based vertex-to-vertex distance), together with the movie “*The Eye*” (vertex-to-hyperedge distance), that is the closest movie to Barry Mendel produced by Yuet-Jan Hui. These suggestions seem legitimate, as Mendel is known for “*The Sixth Sense*”, a mystery drama featuring a boy able to communicate with spirits, while “*The Eye*” is a mystery horror featuring a violinist who sees dead people.

6.5 Approximate s -closeness Centrality

It has been shown that well-connected proteins in PPI networks are more likely to play crucial roles in cellular functions [36]. Thus, several works have proposed to use centrality measures to detect relevant genes and drug targets [68, 47, 41, 76].

We evaluate the ability of HYPED to approximate the s -closeness centrality of vertices and hyperedges in the four PPI hypergraphs in Table 4. For a hyperedge e in a s -connected component c_s , the s -closeness centrality of e is $cl(e, s, c_s) = \sum_{f \in c_s} \Delta_s(e, f) / (|c_s| - 1)$. For a vertex v belonging to a set of hyperedges e_1, \dots, e_p in the s -connected components c_s^1, \dots, c_s^p , the s -closeness centrality of v is $\max_j cl(e_j, s, c_s^j)$.⁶ We use *max* to give more importance to vertices appearing only in large s -connected components than to those belonging to many trivial s -connected components, although other aggregation functions can be used.

Table 9 reports the MAPE and LAR for HYPED-100 in computing the s -closeness centrality of 100 random vertices (v) and hyperedges (h) in each PPI dataset. Both are measures of relative accuracy: MAPE measures the mean absolute percentage error, while LAR [74] is the sum of squares of the log of the accuracy ratio. Due to the hypergraph fragmentation at larger s , vertices likely belong to small s -connected components.

Thanks to the procedure used by HYPED to approximate the s -distances in small components, the centrality of such vertices is well approximated (vertex centrality is defined as a *max*). Thus, we observe smaller errors for vertices than hyperedges. When increasing s , the error usually increases, because the hypergraph becomes more fragmented. The error is low in all but

⁶In contrast to hyperedges, for $s > 1$, a vertex v may belong to different s -connected components, as it may be in hyperedges that overlap only in v .

Table 9: MAPE and LAR for HYPED, in computing the centrality of vertices (v) and hyperedges (h) in the PPI datasets.

Dataset	s	v		h	
		MAPE	LAR	MAPE	LAR
chem-gene	2	0.6077	0.2540	0.5645	0.2218
	3	0.5929	0.2557	0.3866	0.1230
dis-function	2	0.0098	0.0027	0.1376	0.0292
	3	0.0107	0.0020	0.2181	0.0567
dis-gene	2	0.0840	0.0065	0.1795	0.0347
	3	0.0474	0.0021	0.0986	0.0130
dis-chemical	2	0.0096	0.0002	0.2610	0.0753
	3	0.0107	0.0002	0.2857	0.0868

the chem-gene dataset, hence proving the ability of HYPED in accurately approximating the s -closeness centrality of both vertices and hyperedges, in the case of higher-order PPIs. The higher error in chem-gene is due to its higher-order organization, and in particular, to the presence of a big s -connected component with few hubs, and many vertices with low centrality. In such cases, more landmarks are needed to better approximate the centrality, as each landmark is likely to be on only a few shortest s -paths.

7 Conclusions and future work

This paper introduces HYPED, an oracle for point-to-point distance queries in hypergraphs. Our definition of distance includes a parameter s to tune the required level of overlap for two hyperedges to be considered adjacent. Higher values of s emphasize stronger relations between the entities. This strength comes with additional challenges, which require targeted solutions beyond the application of general-purpose graph-based algorithms.

We first presented an oracle based on (i) creating an augmented line graph of the hypergraph, and (ii) building on top of it any state-of-the-art distance oracle for standard graphs. We discussed several important limitations of this approach, and thus proposed a method based on landmarks to produce an accurate oracle with a predefined size directly on the hypergraph. As a side—yet important—contribution, we devised an efficient algorithm for computing the s -connected components of a hypergraph. The experimental comparison with state-of-the-art exact solutions showed that our framework (i) can answer queries as efficiently, even if they trade space

for time; and (ii) can be constructed as efficiently, even though it requires finding all the s -connected components of the hypergraph.

To the best of our knowledge, this is the first work to propose point-to-point distance query oracles in hypergraphs, as well as to propose an algorithm for computing s -connected components in hypergraphs.

Our framework distinguishes itself by handling vertex-to-vertex s -distance queries, a key aspect in measuring proximity within a hypergraph while considering the strength of relations between hyperedges. This is exemplified in scenarios such as song recommendation, where higher values of s lead to more targeted suggestions based on direct connections, while lower values of s promote serendipity by exploring more indirect links between songs. By looking at the top- k s -reachable vertices from a given song, we can offer diverse yet consistent song recommendations.

We emphasize the distinction between vertex-to-vertex s -distance in the hypergraph and hyperedge-to-hyperedge s -distance in its dual hypergraph. An s -path in the hypergraph is a sequence of hyperedges with consecutive hyperedges sharing at least s common vertices, whereas an s -path in the dual hypergraph is a sequence of vertices with consecutive vertices belonging to at least s common hyperedges. As a result, vertices that are s -connected in the hypergraph may not be s -connected in the dual hypergraph. Both definitions hold relevance and may cater to different requirements of the specific application scenario. The ability of our framework to compute both types of distances provides users with a comprehensive toolset for making informed decisions based on their specific objectives.

The current work is just a first step in a new area and opens several avenues for further investigation. Similar to the wide literature on distance oracles in graphs, new different methods can be tried for the same problem we introduced, and specialized approaches can be devised for hypergraphs having specific characteristics, or emerging in specific application domains.

For instance, one could consider hypergraphs where each hyperedge has the same cardinality, or, in dynamic settings, the problem of maintaining the oracle incrementally as the underlying hypergraph evolves.

References

- [1] Hypergraph with sampling for image retrieval. *Pattern Recognition*, 44(10):2255–2262, 2011.
- [2] Takuya Akiba, Yoichi Iwata, and Yuichi Yoshida. Fast exact shortest-

- path distance queries on large networks by pruned landmark labeling. In *SIGMOD*, pages 349–360, 2013.
- [3] Sinan G Aksoy, Cliff Joslyn, Carlos Ortiz Marrero, Brenda Praggastis, and Emilie Purvine. Hypernetwork science via high-order hypergraph walks. *EPJ Data Science*, 9(1):16, 2020.
 - [4] Giorgio Ausiello and Luigi Laura. Directed hypergraphs: Introduction and fundamental algorithms—a survey. *Theoretical Computer Science*, 658:293–306, 2017.
 - [5] Surender Baswana, Vishrut Goyal, and Sandeep Sen. All-pairs nearly 2-approximate shortest paths in $o(n^2 \text{polylog} n)$ time. *Theoretical Computer Science*, 410(1):84–93, 2009.
 - [6] Austin R Benson, Rediet Abebe, Michael T Schaub, Ali Jadbabaie, and Jon Kleinberg. Simplicial closure and higher-order link prediction. *PNAS*, 115(48):E11221–E11230, 2018.
 - [7] Claude Berge. *Hypergraphs: combinatorics of finite sets*, volume 45. Elsevier, 1984.
 - [8] Nadja Betzler, Michael R Fellows, Jiong Guo, Rolf Niedermeier, and Frances A Rosamond. Fixed-parameter algorithms for kemeny scores. In *AAIM*, pages 60–71, 2008.
 - [9] Jacob Charles Wright Billings, Mirko Hu, Giulia Lerda, Alexey N Medvedev, Francesco Mottes, Adrian Onicas, Andrea Santoro, and Giovanni Petri. Simplex2vec embeddings for community detection in simplicial complexes. *arXiv preprint arXiv:1906.09068*, 2019.
 - [10] Bryan Brancotte, Bo Yang, Guillaume Blin, Sarah Cohen-Boulakia, Alain Denise, and Sylvie Hamel. Rank aggregation with ties: Experiments and analysis. *PVLDB*, 8(11):1202–1213, 2015.
 - [11] Alain Bretto, Hocine Cherifi, and Driss Aboutajdine. Hypergraph imaging: an overview. *Pattern Recognition*, 35(3):651–658, 2002.
 - [12] Jiajun Bu, Shulong Tan, Chun Chen, Can Wang, Hao Wu, Lijun Zhang, and Xiaofei He. Music recommendation by unified hypergraph: Combining social media information and music content. In *MM*, pages 391–400, 2010.

- [13] Eden Chlamtác, Michael Dinitz, Christian Konrad, Guy Kortsarz, and George Rabanca. The densest k -subhypergraph problem. *SIAM Journal on Discrete Mathematics*, 32(2):1458–1477, 2018.
- [14] Sarah Cohen-Boulakia, Alain Denise, and Sylvie Hamel. Using medians to generate consensus rankings for biological data. In *SSDBM*, pages 73–90, 2011.
- [15] Oliver Cooley, Mihyun Kang, and Christoph Koch. Evolution of high-order connected components in random hypergraphs. *Electronic Notes in Discrete Mathematics*, 49:569–575, 2015.
- [16] Colin Cooper, Sang Hyuk Lee, Tomasz Radzik, and Yiannis Siantos. Random walks in recommender systems: exact computation and simulations. In *WWW*, pages 811–816, 2014.
- [17] Luis F De Figueiredo, Stefan Schuster, Christoph Kaleta, and David A Fell. Can sugars be produced from fatty acids? a test case for pathway analysis tools. *Bioinformatics*, 24(22):2615–2621, 2008.
- [18] Richard Draves, Jitendra Padhye, and Brian Zill. Routing in multi-radio, multi-hop wireless mesh networks. In *MobiCom*, pages 114–128, 2004.
- [19] Muhammad Farhan, Qing Wang, Yu Lin, and Brendan McKay. A highly scalable labelling approach for exact distance queries in complex networks. *EDBT*, 2019.
- [20] Bahare Fatemi, Perouz Taslakian, David Vazquez, and David Poole. Knowledge hypergraphs: Prediction beyond binary relations. *arXiv preprint arXiv:1906.00137*, 2019.
- [21] Song Feng, Emily Heath, Brett Jefferson, Cliff Joslyn, Henry Kvinge, Hugh D Mitchell, Brenda Praggastis, Amie J Einfeld, Amy C Sims, Larissa B Thackray, et al. Hypergraph models of biological networks to identify genes critical to pathogenic viral response. *BMC bioinformatics*, 22(1):1–21, 2021.
- [22] Yifan Feng, Haoxuan You, Zizhao Zhang, Rongrong Ji, and Yue Gao. Hypergraph neural networks. In *AAAI*, pages 3558–3565, 2019.
- [23] Nicholas Franzese, Adam Groce, TM Murali, and Anna Ritz. Hypergraph-based connectivity measures for signaling pathway topologies. *PLoS computational biology*, 15(10):e1007384, 2019.

- [24] Giorgio Gallo, Giustino Longo, Stefano Pallottino, and Sang Nguyen. Directed hypergraphs and applications. *Discrete Applied Mathematics*, 42(2-3):177–201, 1993.
- [25] Jianhang Gao, Qing Zhao, Wei Ren, Ananthram Swami, Ram Ramanathan, and Amotz Bar-Noy. Dynamic shortest path algorithms for hypergraphs. *Transactions on Networking*, 23(6):1805–1817, 2014.
- [26] Andrew V Goldberg. Point-to-point shortest path algorithms with pre-processing. In *SOFSEM*, pages 88–102, 2007.
- [27] Andrew V Goldberg and Chris Harrelson. Computing the shortest path: A search meets graph theory. In *SODA*, volume 5, pages 156–165. Citeseer, 2005.
- [28] Andrew V Goldberg, Haim Kaplan, and Renato F Werneck. Reach for a*: Efficient point-to-point shortest path algorithms. In *ALENEX*, pages 129–143. SIAM, 2006.
- [29] Roy Goldman, Narayanan Shivakumar, Suresh Venkatasubramanian, and Hector Garcia-Molina. Proximity search in databases. In *VLDB*, volume 98, pages 26–37, 1998.
- [30] Marco Gori and Augusto Pucci. Research paper recommender systems: A random-walk based approach. In *2006 IEEE/WIC/ACM International Conference on Web Intelligence (WI 2006 Main Conference Proceedings)(WI’06)*, pages 778–781, 2006.
- [31] Marco Gori, Augusto Pucci, Via Roma, and I Siena. Itemrank: A random-walk based scoring algorithm for recommender engines. In *IJCAI*, volume 7, pages 2766–2771, 2007.
- [32] Andrey Gubichev, Srikanta Bedathur, Stephan Seufert, and Gerhard Weikum. Fast and accurate estimation of shortest paths in large graphs. In *CIKM*, pages 499–508, 2010.
- [33] Jin Huang, Rui Zhang, and Jeffrey Xu Yu. Scalable hypergraph learning and processing. In *ICDM*, pages 775–780, 2015.
- [34] Hyunjin Hwang, Seungwoo Lee, and Kijung Shin. Hyfer: A framework for making hypergraph learning easy, scalable and benchmarkable. In *GLB*, 2021.

- [35] Giuseppe F Italiano and Umberto Nanni. Online maintenance of minimal directed hypergraphs. 1989.
- [36] Hawoong Jeong, Sean P Mason, A-L Barabási, and Zoltan N Oltvai. Lethality and centrality in protein networks. *Nature*, 411(6833):41–42, 2001.
- [37] Shuyi Ji, Yifan Feng, Rongrong Ji, Xibin Zhao, Wanwan Tang, and Yue Gao. Dual channel hypergraph collaborative filtering. In *KDD*, pages 2020–2029, 2020.
- [38] Jianwen Jiang, Yuxuan Wei, Yifan Feng, Jingxuan Cao, and Yue Gao. Dynamic hypergraph neural networks. In *IJCAI*, pages 2635–2641, 2019.
- [39] Ruoming Jin, Zhen Peng, Wendell Wu, Feodor Dragan, Gagan Agrawal, and Bin Ren. Parallelizing pruned landmark labeling: dealing with dependencies in graph algorithms. In *ICS*, pages 1–13, 2020.
- [40] Cliff A Joslyn, Sinan G Aksoy, Tiffany J Callahan, Lawrence E Hunter, Brett Jefferson, Brenda Praggastis, Emilie Purvine, and Ignacio J Tripodi. Hypernetwork science: from multidimensional networks to computational topology. In *CCS*, pages 377–392, 2020.
- [41] Maliackal Poulo Joy, Amy Brock, Donald E Ingber, and Sui Huang. High-betweenness proteins in the yeast protein interaction network. *Journal of Biomedicine and Biotechnology*, 2005(2):96, 2005.
- [42] G. Karypis, R. Aggarwal, V. Kumar, and S. Shekhar. Multilevel hypergraph partitioning: applications in vlsi domain. *VLSI*, 7(1):69–79, 1999.
- [43] John G Kemeny. Mathematics without numbers. *Daedalus*, 88(4):577–591, 1959.
- [44] Steve Kirkland. Two-mode networks exhibiting data loss. *Journal of Complex Networks*, 6(2):297–316, 2018.
- [45] Steffen Klamt, Utz-Uwe Haus, and Fabian Theis. Hypergraphs and cellular networks. *PLoS computational biology*, 5(5):e1000385, 2009.
- [46] Jon M Kleinberg. Navigation in a small world. *Nature*, 406(6798):845–845, 2000.

- [47] Max Kotlyar, Kristen Fortney, and Igor Jurisica. Network-based characterization of drug-regulated genes, drug targets, and toxicity. *Methods*, 57(4):499–507, 2012.
- [48] Spencer Krieger and John Kececioglu. Fast approximate shortest hyperpaths for inferring pathways in cell signaling hypergraphs. In *WABI. Schloss Dagstuhl-Leibniz-Zentrum für Informatik*, 2021.
- [49] Ravi Kumar and Sergei Vassilvitskii. Generalized distances between rankings. In *WWW*, pages 571–580, 2010.
- [50] Dong Li, Zhiming Xu, Sheng Li, and Xin Sun. Link prediction in social networks based on hypergraph. In *WWW*, pages 41–42, 2013.
- [51] Jianbo Li, Jingrui He, and Yada Zhu. E-tail product return prediction via hypergraph-based local graph cut. In *KDD*, pages 519–527, 2018.
- [52] Wentao Li, Miao Qiao, Lu Qin, Ying Zhang, Lijun Chang, and Xuemin Lin. Scaling up distance labeling on graphs with core-periphery properties. In *SIGMOD*, pages 1367–1381, 2020.
- [53] Xu T Liu, Jesun Firoz, Sinan Aksoy, Ilya Amburg, Andrew Lumsdaine, Cliff Joslyn, Assefaw H Gebremedhin, and Brenda Praggastis. High-order line graphs of non-uniform hypergraphs: Algorithms, applications, and experimental analysis. *arXiv preprint arXiv:2201.11326*, 2022.
- [54] Xu T Liu, Jesun Firoz, Andrew Lumsdaine, Cliff Joslyn, Sinan Aksoy, Brenda Praggastis, and Assefaw Gebremedhin. Parallel algorithms and heuristics for efficient computation of high-order line graphs of hypergraphs. *arXiv preprint arXiv:2010.11448*, 2020.
- [55] Linyuan Lu and Xing Peng. High-ordered random walks and generalized laplacians on hypergraphs. In *International Workshop on Algorithms and Models for the Web-Graph*, pages 14–25, 2011.
- [56] Qi Luo, Dongxiao Yu, Zhipeng Cai, Xuemin Lin, Guanghui Wang, and Xiuzhen Cheng. Toward maintenance of hypercores in large-scale dynamic hypergraphs. *VLDBJ*, pages 1–18, 2022.
- [57] Fredrik Manne, Md Patwary, and Mostofa Ali. A scalable parallel union-find algorithm for distributed memory computers. In *PPAM*, pages 186–195, 2009.

- [58] Lars Relund Nielsen, Kim Allan Andersen, and Daniele Pretolani. Finding the k shortest hyperpaths. *Computers & operations research*, 32(6):1477–1497, 2005.
- [59] Michalis Potamias, Francesco Bonchi, Carlos Castillo, and Aristides Gionis. Fast shortest path distance estimation in large networks. In *CIKM*, pages 867–876, 2009.
- [60] Giulia Preti, Gianmarco De Francisci Morales, and Francesco Bonchi. Strud: Truss decomposition of simplicial complexes. In *The Web Conference*, pages 3408–3418, 2021.
- [61] Zichao Qi, Yanghua Xiao, Bin Shao, and Haixun Wang. Toward a distance oracle for billion-node graphs. *PVLDB*, 7(1):61–72, 2013.
- [62] Syed Asad Rahman, P Advani, R Schunk, Rainer Schrader, and Dietmar Schomburg. Metabolic pathway analysis web service (pathway hunter tool at cubic). *Bioinformatics*, 21(7):1189–1193, 2005.
- [63] Anna Ritz, Brendan Avent, and TM Murali. Pathway analysis with signaling hypergraphs. *TCBB*, 14(5):1042–1055, 2015.
- [64] Anna Ritz, Allison N Tegge, Hyunju Kim, Christopher L Poirel, and TM Murali. Signaling hypergraphs. *Trends in biotechnology*, 32(7):356–362, 2014.
- [65] Bernhard Schölkopf, John Platt, and Thomas Hofmann. Learning with hypergraphs: Clustering, classification, and embedding. In *NIPS*, pages 1601–1608, 2007.
- [66] Julian Shun. Practical parallel hypergraph algorithms. In *SIGPLAN*, pages 232–249, 2020.
- [67] Christian Sommer. Shortest-path queries in static networks. *CSU*, 46(4):1–31, 2014.
- [68] Asma Soofi, Mohammad Taghizadeh, Seyyed Mohammad Tabatabaei, Mostafa Rezaei Tavirani, Heeva Shakib, Saeed Namaki, and Nahid Safari Alighiarloo. Centrality analysis of protein-protein interaction networks and molecular docking prioritize potential drug-targets in type 1 diabetes. *IJPR*, 19(4):121, 2020.
- [69] Binta Sun, T.-H. Hubert Chan, and Mauro Sozio. Fully dynamic approximate k-core decomposition in hypergraphs. *TKDD*, 14(4), 2020.

- [70] Hung-Khoon Tan, Chong-Wah Ngo, and Xiao Wu. Modeling video hyperlinks with hypergraph for web video reranking. In *MM*, pages 659–662, 2008.
- [71] Shulong Tan, Ziyu Guan, Deng Cai, Xuzhen Qin, Jiajun Bu, and Chun Chen. Mapping users across networks by manifold alignment on hypergraph. *AAAI*, 28(1), 2014.
- [72] Robert E Tarjan and Jan Van Leeuwen. Worst-case analysis of set union algorithms. *JACM*, 31(2):245–281, 1984.
- [73] Mikkel Thorup and Uri Zwick. Approximate distance oracles. *JACM*, 52(1):1–24, 2005.
- [74] Chris Tofallis. A better measure of relative prediction accuracy for model selection and model estimation. *Journal of the Operational Research Society*, 66(8):1352–1362, 2015.
- [75] Konstantin Tretyakov, Abel Armas-Cervantes, Luciano García-Bañuelos, Jaak Vilo, and Marlon Dumas. Fast fully dynamic landmark-based estimation of shortest path distances in very large graphs. In *CIKM*, pages 1785–1794, 2011.
- [76] Ariele Viacava Follis. Centrality of drug targets in protein networks. *BMC bioinformatics*, 22(1):1–29, 2021.
- [77] Monique V Vieira, Bruno M Fonseca, Rodrigo Damazio, Paulo B Golgher, Davi de Castro Reis, and Berthier Ribeiro-Neto. Efficient search ranking in social networks. In *CIKM*, pages 563–572, 2007.
- [78] Qiongwen Xu, Xu Zhang, Jin Zhao, Xin Wang, and Tilman Wolf. Fast shortest-path queries on large-scale graphs. In *ICNP*, pages 1–10, 2016.
- [79] Dingqi Yang, Bingqing Qu, Jie Yang, and Philippe Cudre-Mauroux. Revisiting user mobility and social relationships in lbsns: A hypergraph embedding approach. In *WWW*, pages 2147–2157, 2019.
- [80] Muhan Zhang, Zhicheng Cui, Shali Jiang, and Yixin Chen. Beyond link prediction: Predicting hyperlinks in adjacency space. *AAAI*, 32(1), 2018.
- [81] Zizhao Zhang, Yifan Feng, Shihui Ying, and Yue Gao. Deep hypergraph structure learning. *CoRR*, abs/2208.12547, 2022.

- [82] Xiaoyao Zheng, Yonglong Luo, Liping Sun, Xintao Ding, and Ji Zhang. A novel social network hybrid recommender system based on hypergraph topologic structure. *WWW*, pages 985–1013, 2018.
- [83] Yu Zhu, Ziyu Guan, Shulong Tan, Haifeng Liu, Deng Cai, and Xiaofei He. Heterogeneous hypergraph embedding for document recommendation. *Neurocomputing*, 216:150–162, 2016.